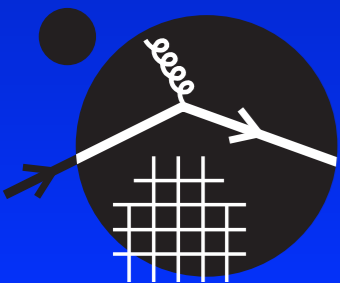
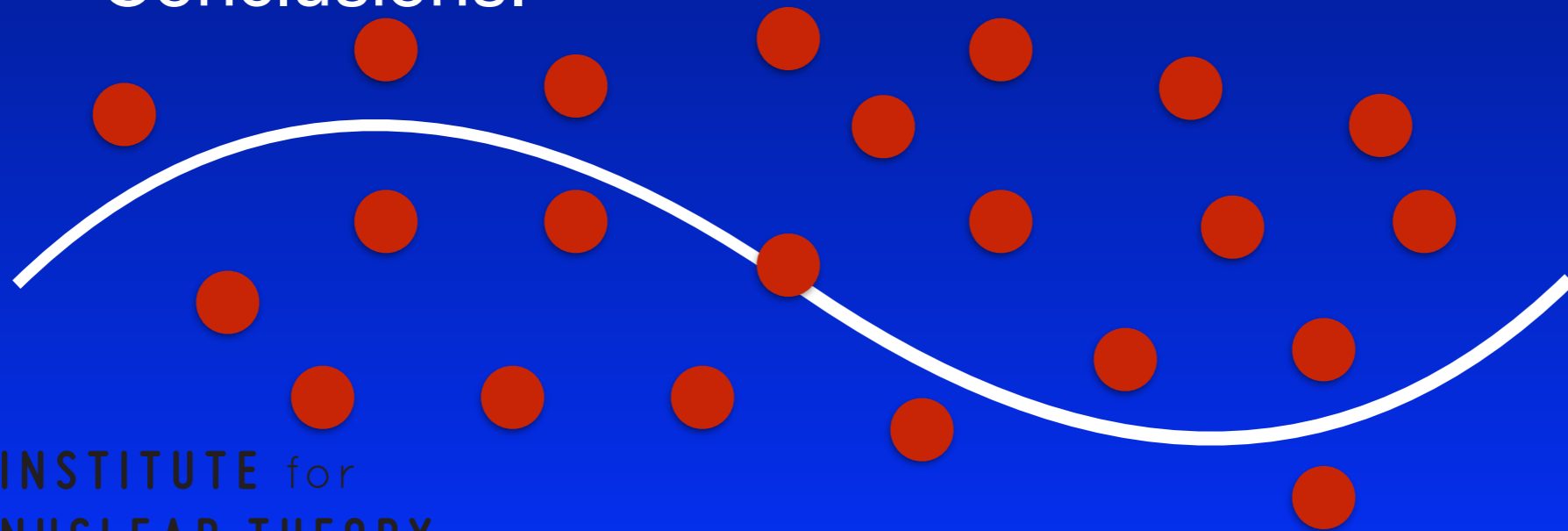


Neutrino interactions in dense matter and implications for astrophysics

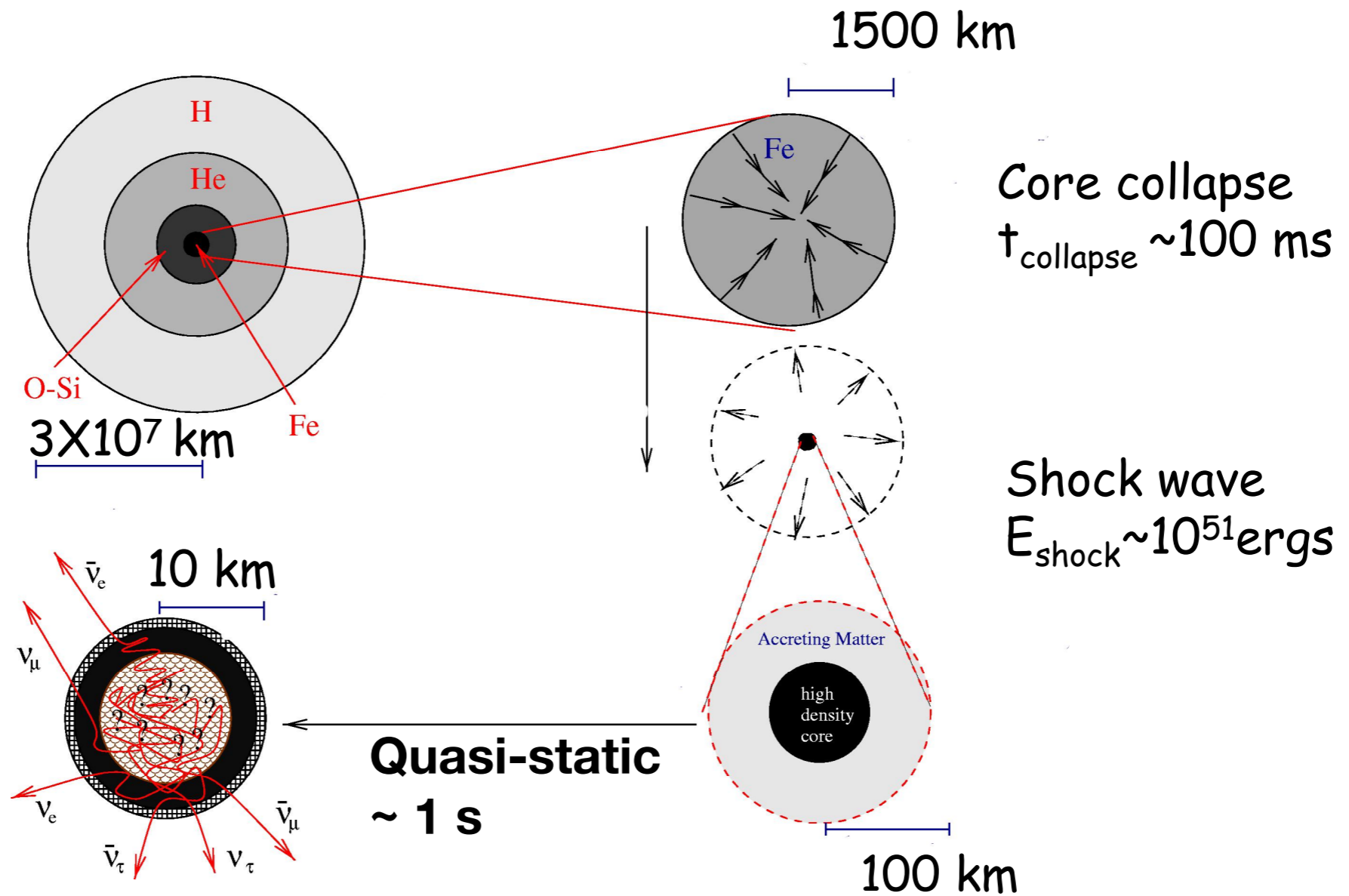
Sanjay Reddy
Univ. of Washington, Seattle

- Motivation
- Preliminaries: linear response & sum rules
- Neutrino scattering at:
 - 10^{12} g/cm³ (neutrino-sphere)
 - 10^{13} g/cm³ (role of nuclei and pasta)
 - 10^{14} g/cm³ (spin response of nuclear matter)
- Conclusions.



INSTITUTE for
NUCLEAR THEORY

Core Collapse Supernova



Energy radiated, mostly in neutrinos : $E_{\text{SN}} \sim \frac{3GM_{\text{pns}}^2}{5r_{\text{NS}}} \approx 3 \times 10^{53} \text{ erg} \left(\frac{M_{\text{pns}}}{M_{\odot}} \right)^2 \left(\frac{r_{\text{NS}}}{12 \text{ km}} \right)^{-1}$

Lepton number radiated, also in neutrinos : $N_L \approx 3.4 \times 10^{56} \left(\frac{M_{\text{pns}}}{1.4 M_{\odot}} \right)$

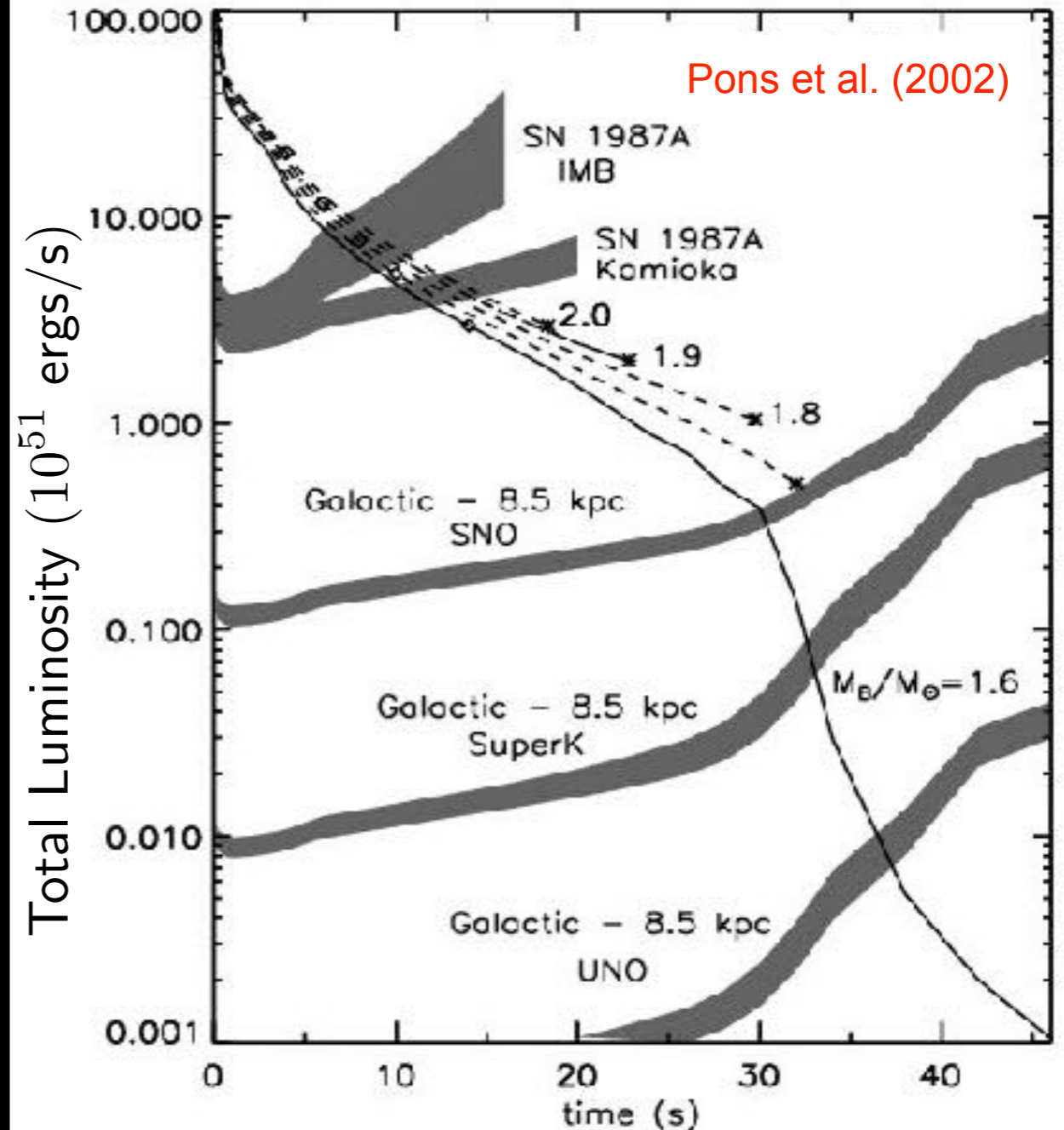
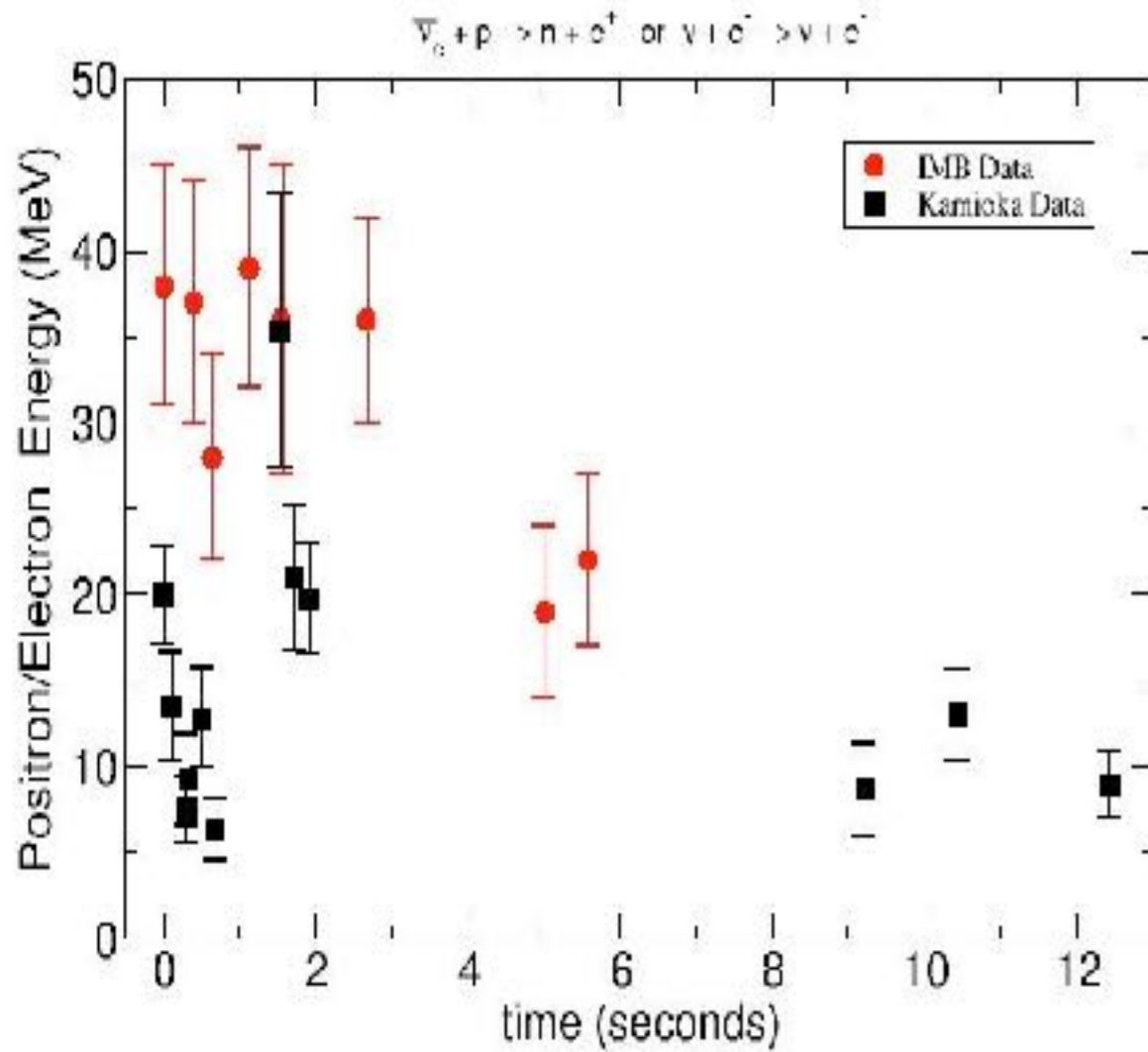
Timescale and energy spectrum of neutrinos is set by neutrino interactions in the hot newly born neutron star

Supernova Neutrinos

3×10^{53} ergs = $10^{58} \times 20$ MeV Neutrinos

SN 1987a: ~ 20 neutrinos in support of supernova theory

SuperK can detect ~10,000 neutrinos from a galactic supernova at 10 kpc



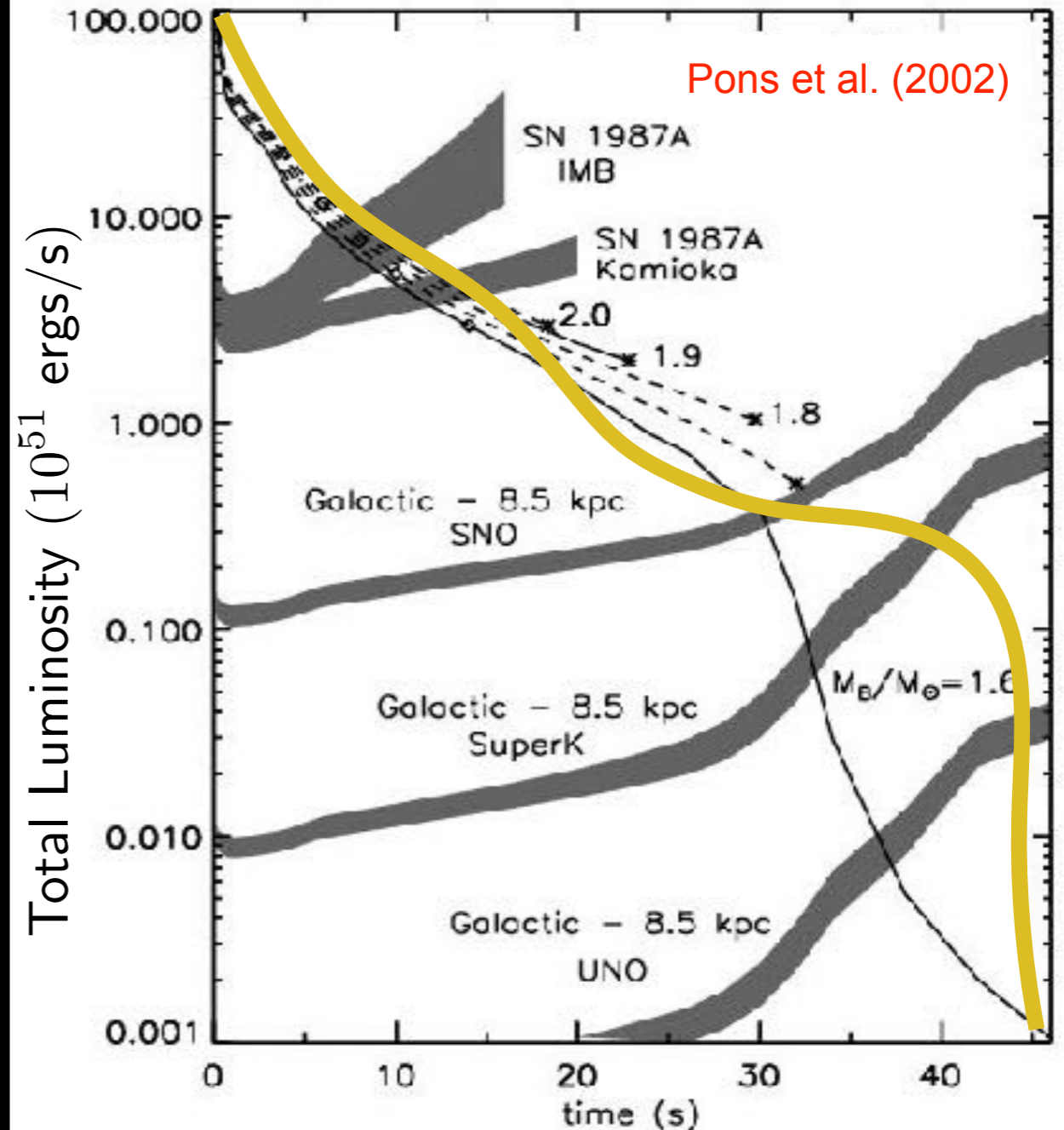
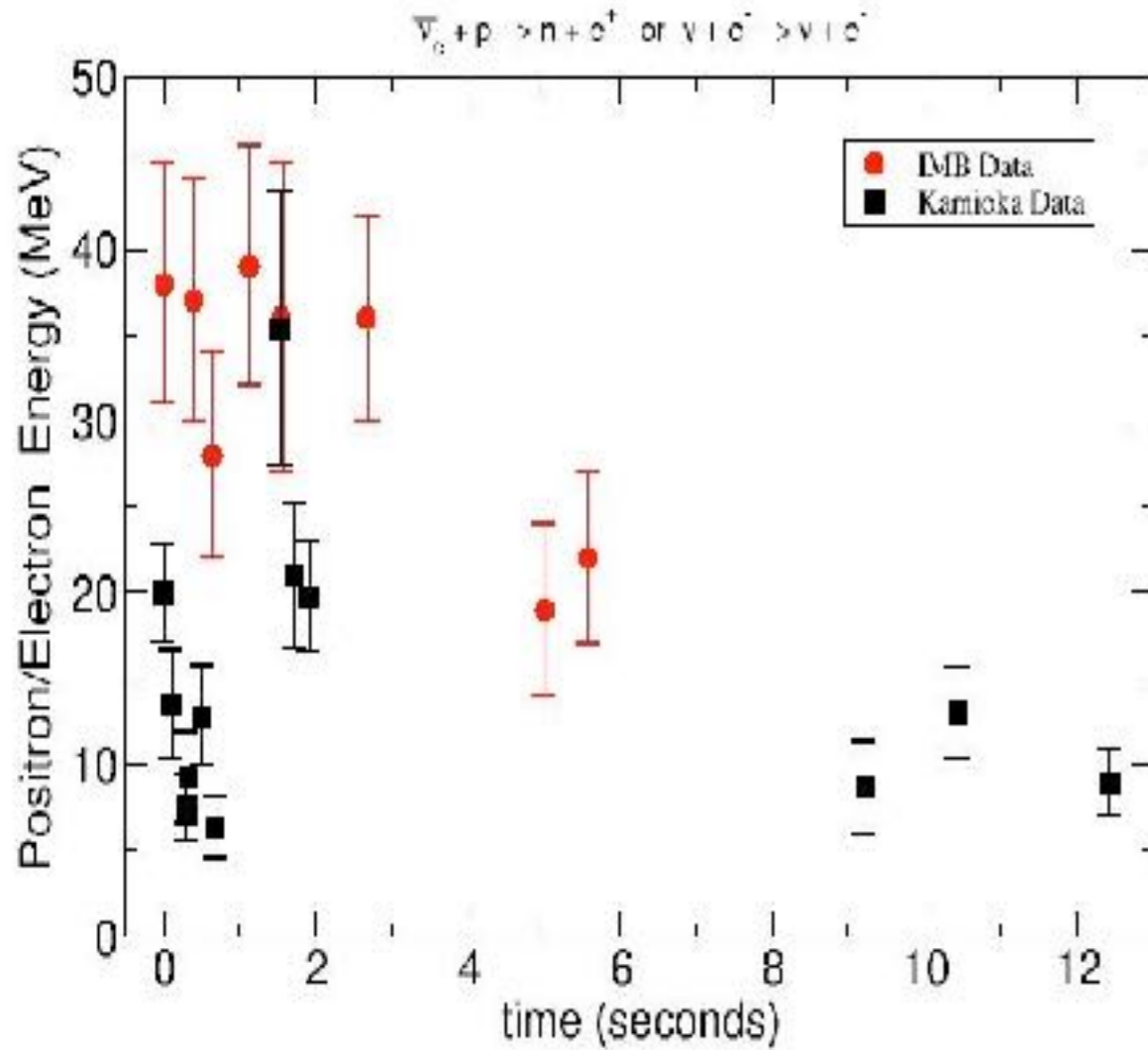
$$\frac{dN_{\text{detect}}}{dt} \approx \frac{\sigma_{\text{ref}} \times n_p \times M_{\text{tons}}}{4\pi D^2} \frac{E_\nu^2}{m_e^2} \frac{dN_{\text{emit}}}{dt}$$

Supernova Neutrinos

3×10^{53} ergs = $10^{58} \times 20$ MeV Neutrinos

SN 1987a: ~ 20 neutrinos in support of supernova theory

SuperK can detect ~10,000 neutrinos from a galactic supernova at 10 kpc



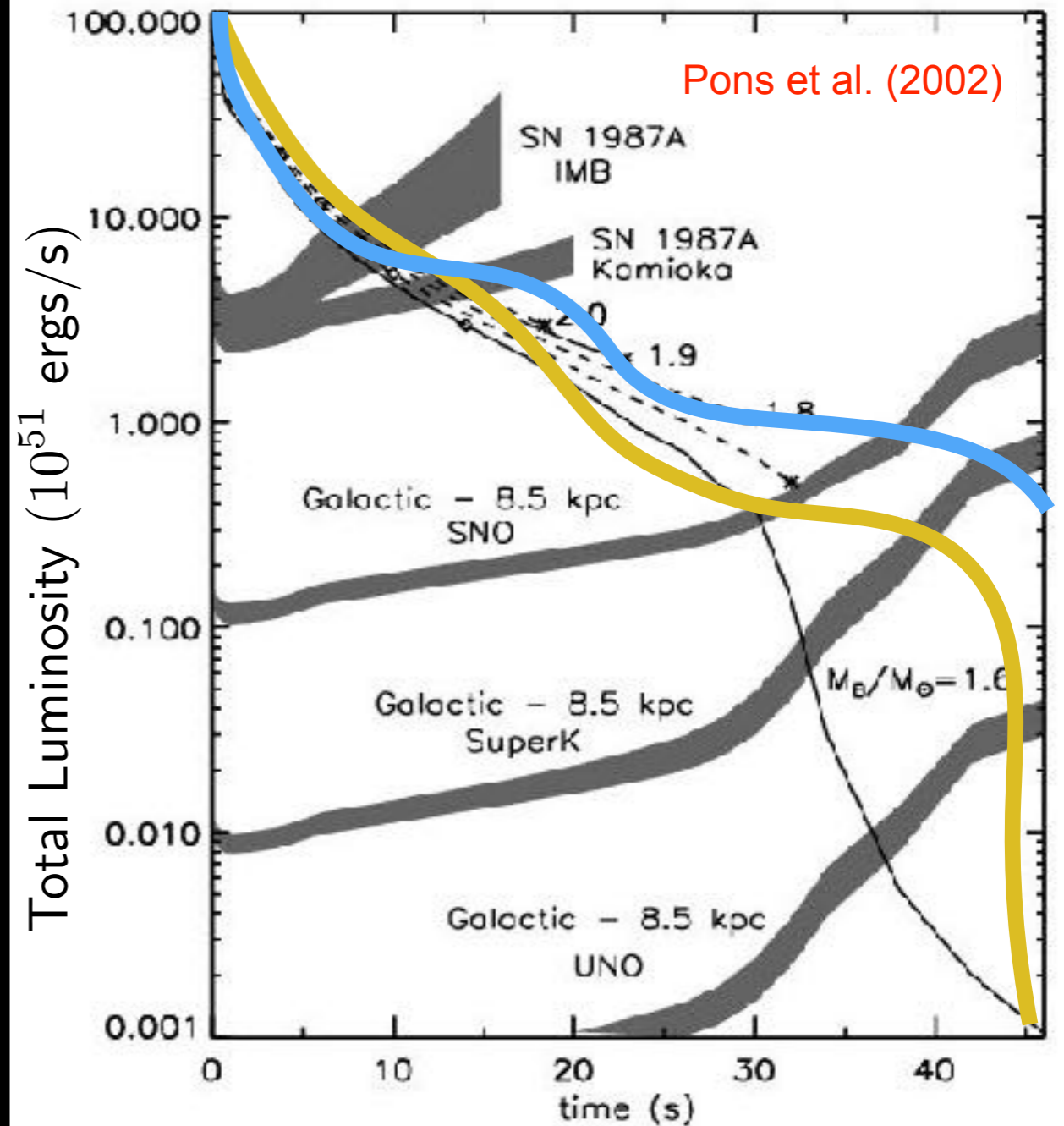
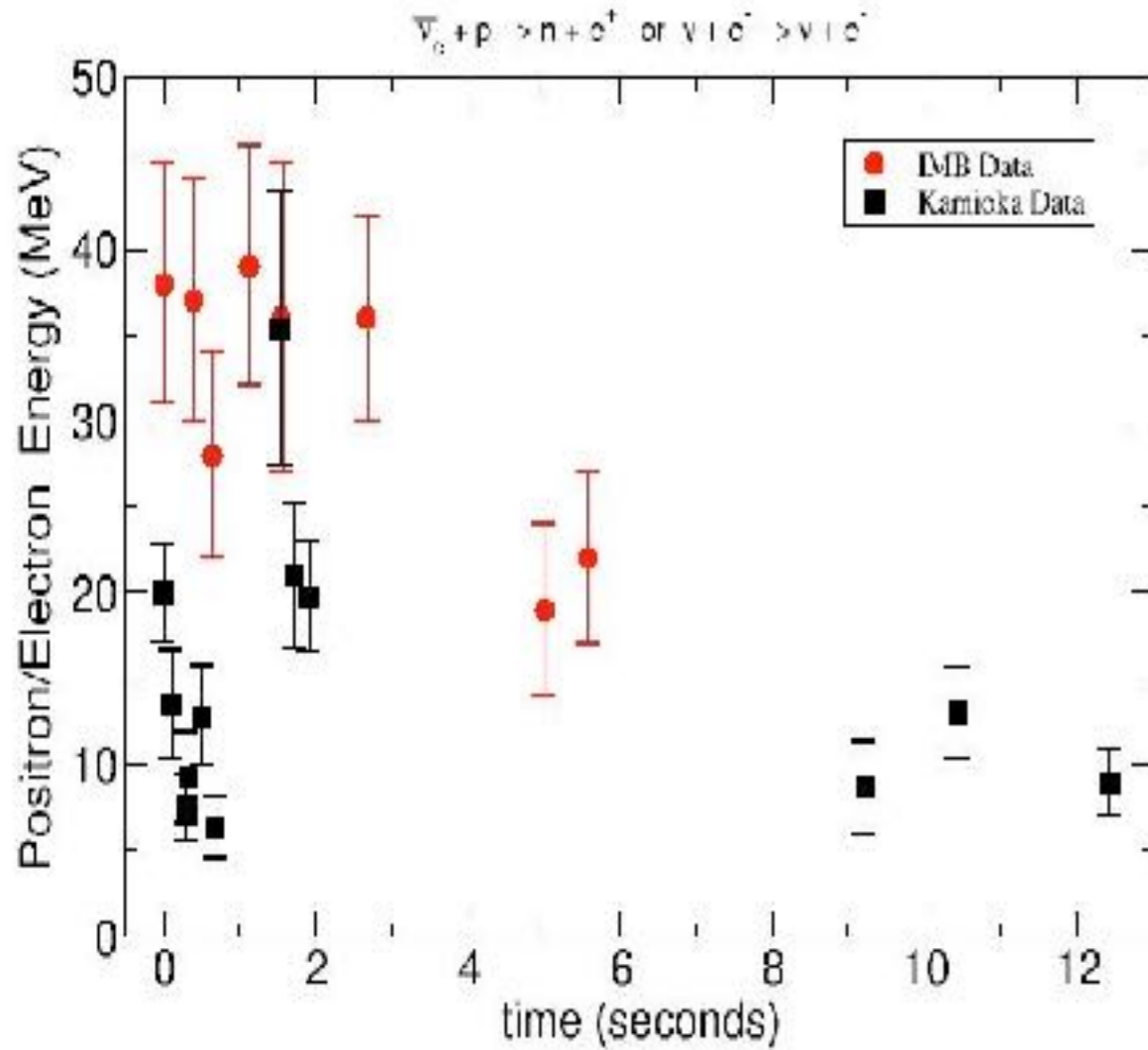
$$\frac{dN_{\text{detect}}}{dt} \approx \frac{\sigma_{\text{ref}} \times n_p \times M_{\text{tons}}}{4\pi D^2} \frac{E_\nu^2}{m_e^2} \frac{dN_{\text{emit}}}{dt}$$

Supernova Neutrinos

3×10^{53} ergs = $10^{58} \times 20$ MeV Neutrinos

SN 1987a: ~ 20 neutrinos in support of supernova theory

SuperK can detect ~10,000 neutrinos from a galactic supernova at 10 kpc



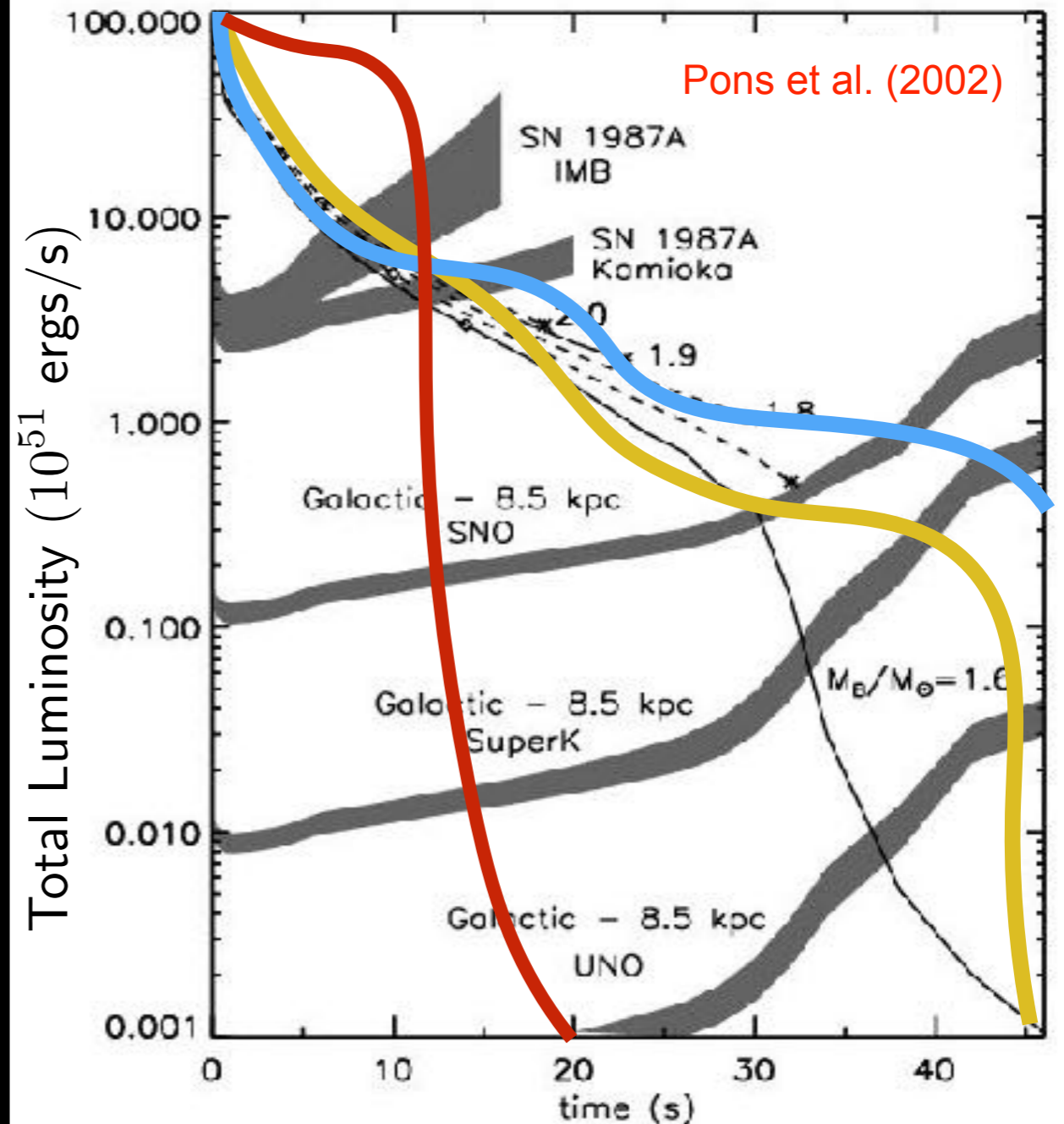
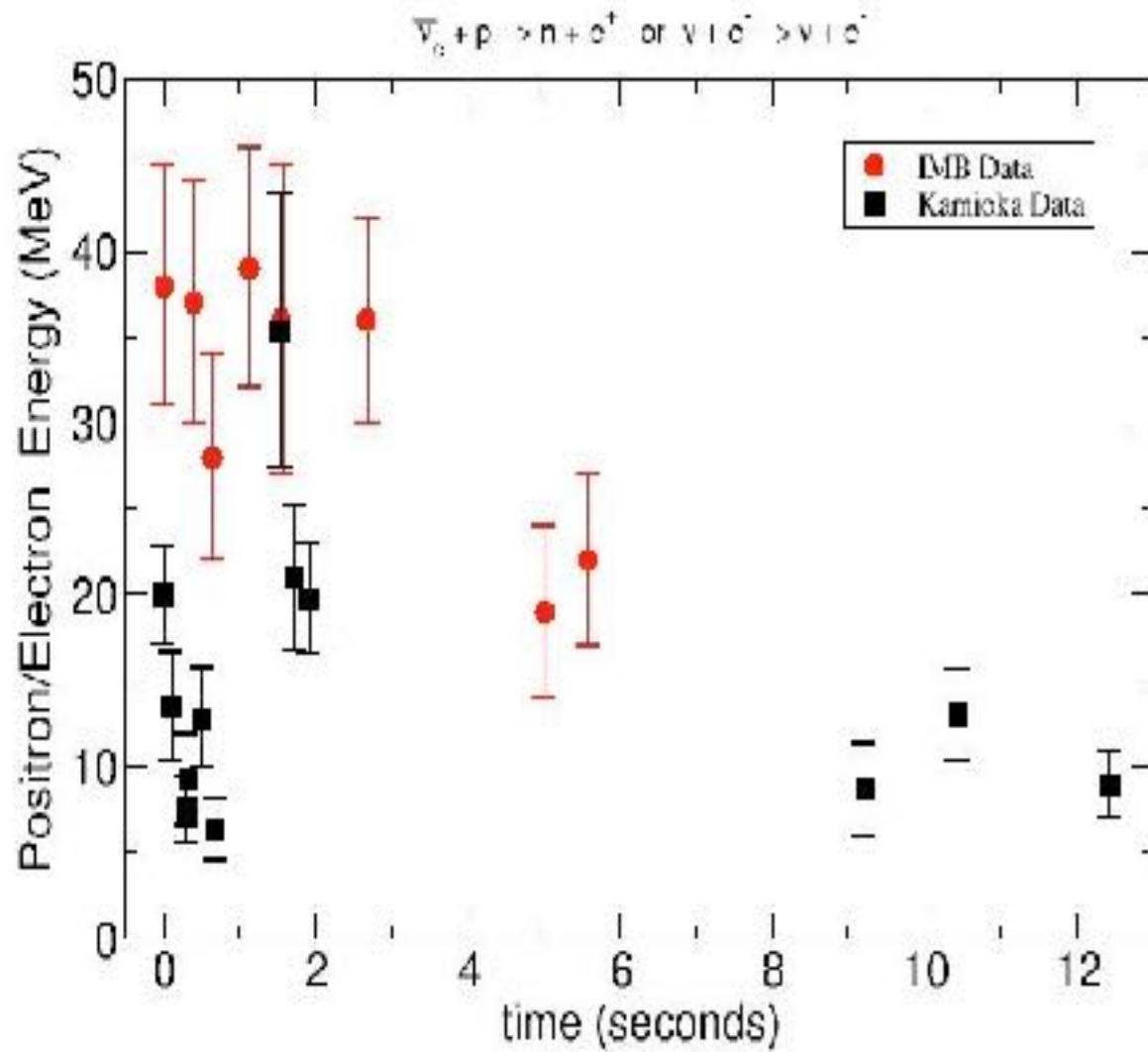
$$\frac{dN_{\text{detect}}}{dt} \approx \frac{\sigma_{\text{ref}} \times n_p \times M_{\text{tons}}}{4\pi D^2} \frac{E_\nu^2}{m_e^2} \frac{dN_{\text{emit}}}{dt}$$

Supernova Neutrinos

3×10^{53} ergs = $10^{58} \times 20$ MeV Neutrinos

SN 1987a: ~ 20 neutrinos in support of supernova theory

SuperK can detect ~10,000 neutrinos from a galactic supernova at 10 kpc



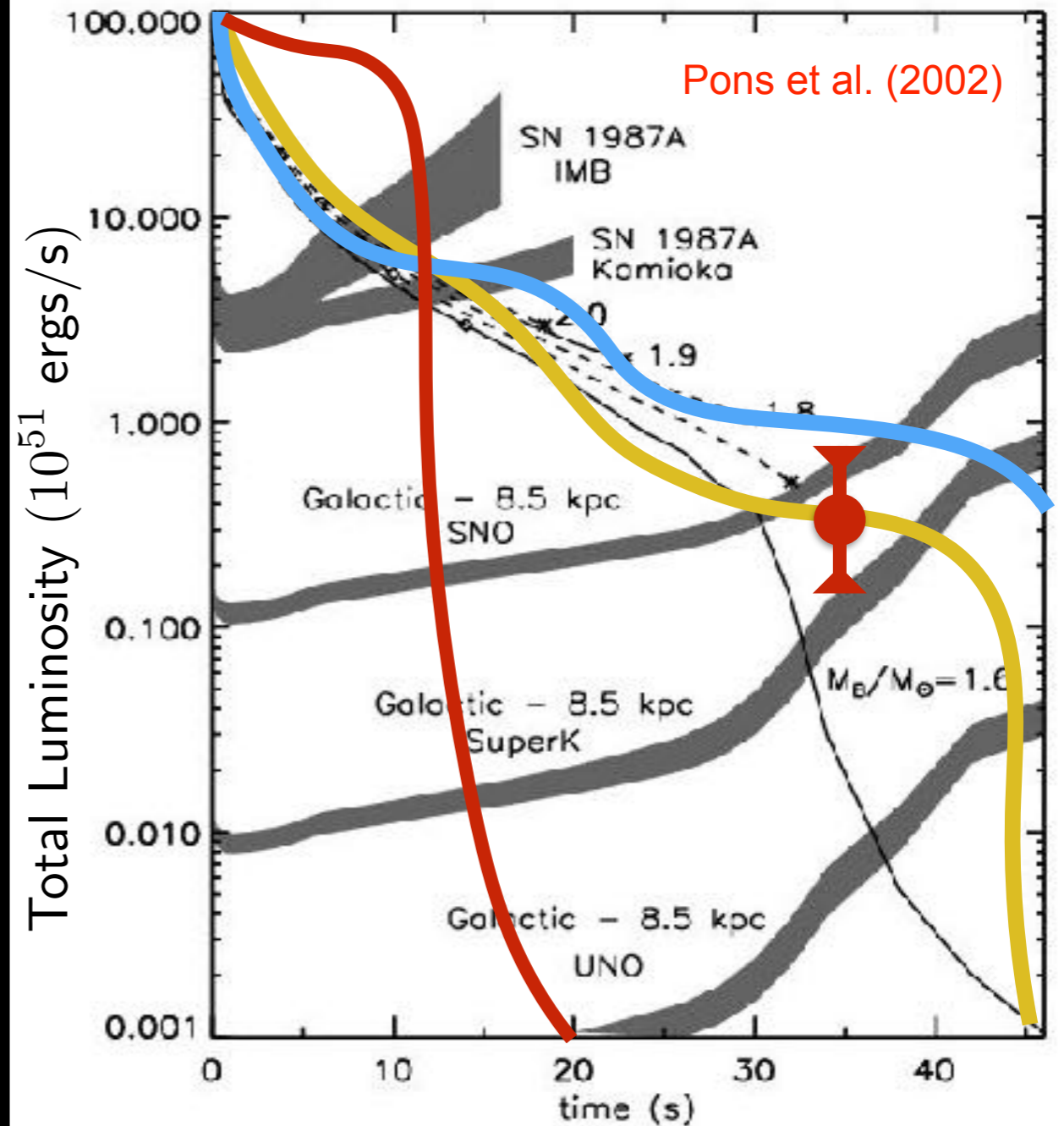
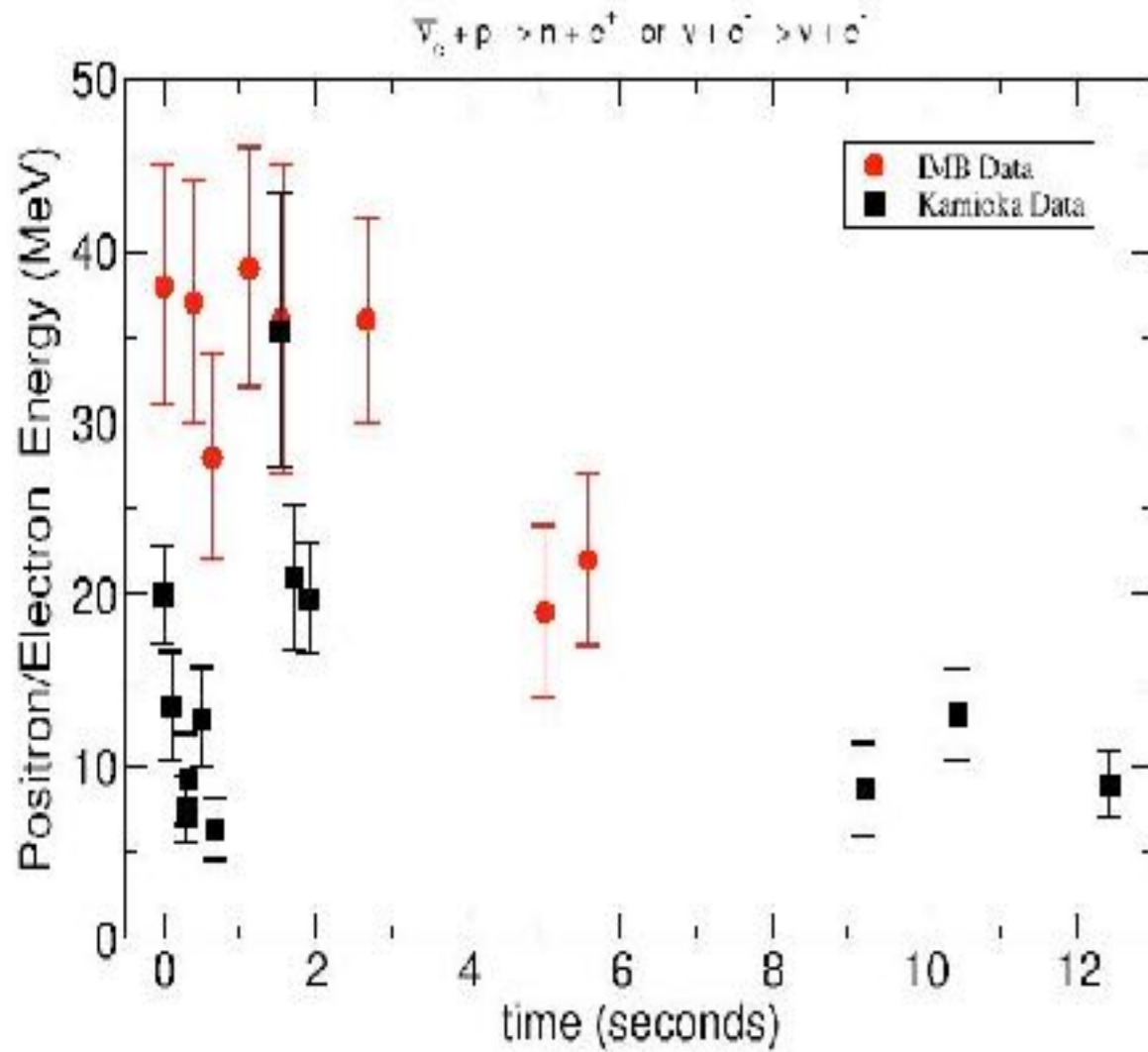
$$\frac{dN_{\text{detect}}}{dt} \approx \frac{\sigma_{\text{ref}} \times n_p \times M_{\text{tons}}}{4\pi D^2} \frac{E_\nu^2}{m_e^2} \frac{dN_{\text{emit}}}{dt}$$

Supernova Neutrinos

3×10^{53} ergs = $10^{58} \times 20$ MeV Neutrinos

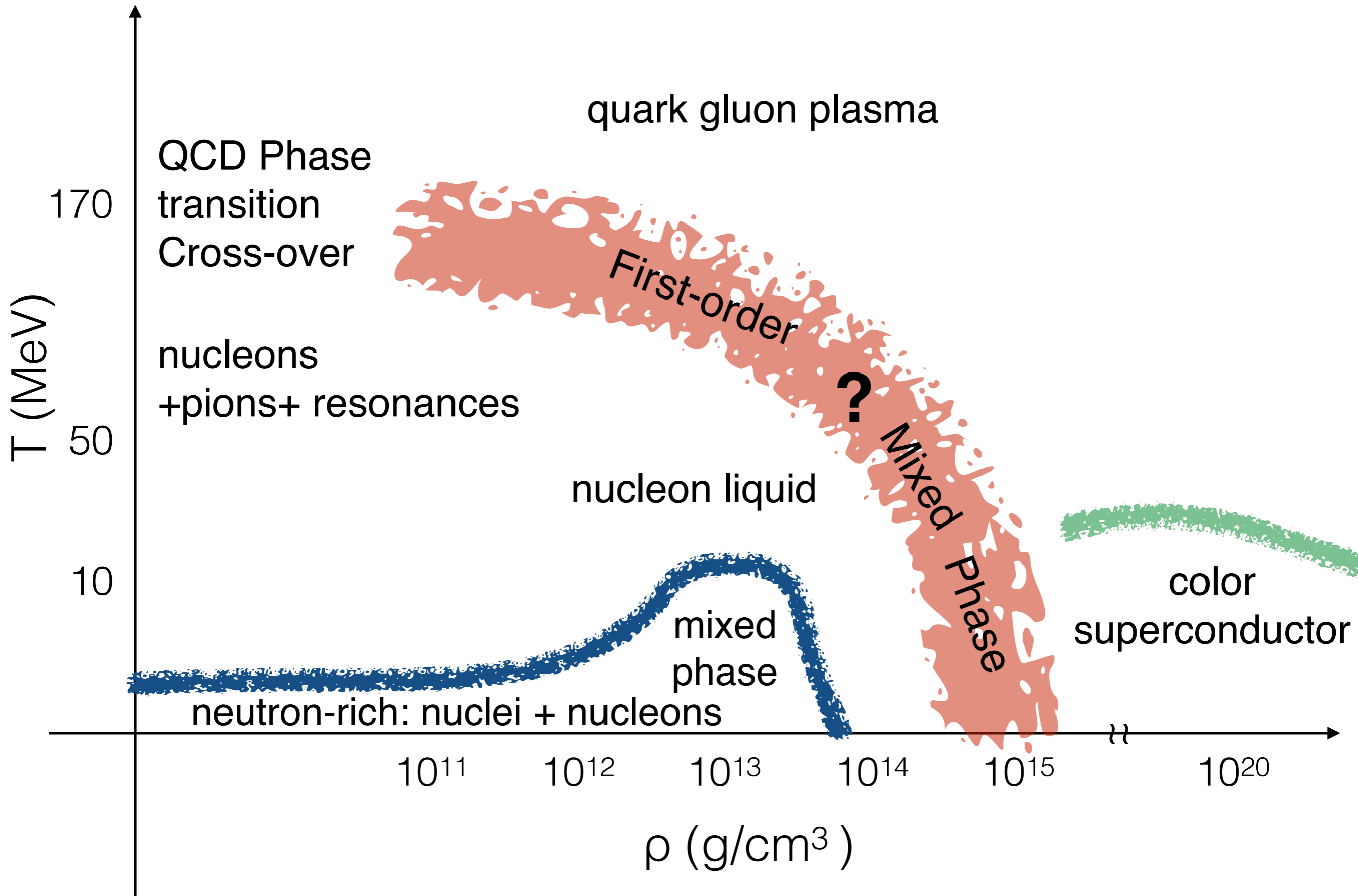
SN 1987a: ~ 20 neutrinos in support of supernova theory

SuperK can detect ~10,000 neutrinos from a galactic supernova at 10 kpc

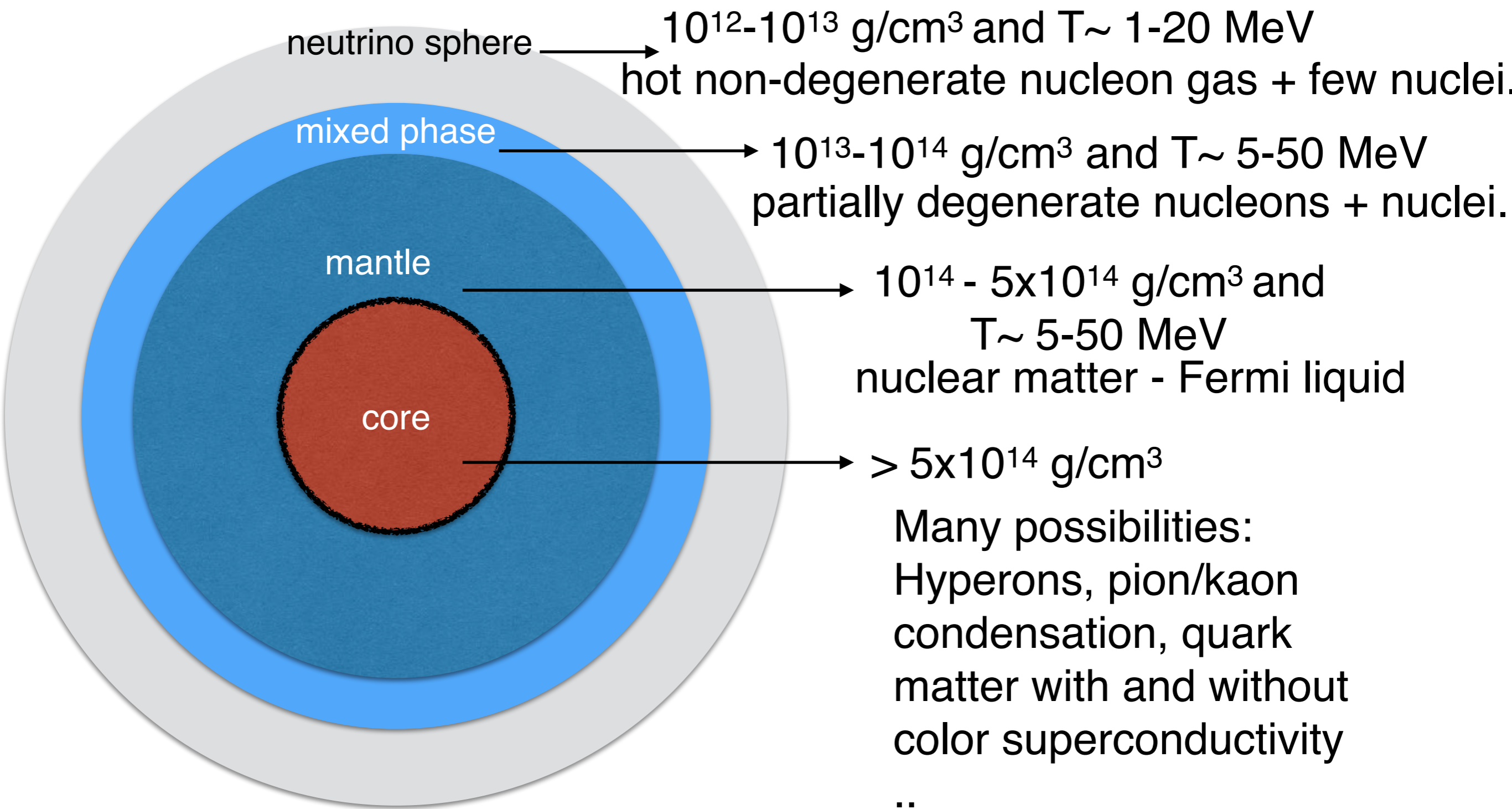


$$\frac{dN_{\text{detect}}}{dt} \approx \frac{\sigma_{\text{ref}} \times n_p \times M_{\text{tons}}}{4\pi D^2} \frac{E_\nu^2}{m_e^2} \frac{dN_{\text{emit}}}{dt}$$

Phase Diagram of Hot and Dense Matter



Neutrino Scattering in Hot Neutron Stars



Neutrino Interactions in Dense Matter

Low energy Lagrangian: $\mathcal{L} = \frac{G_F}{\sqrt{2}} l_\mu j^\mu \quad l_1 + N_2 \rightarrow l_3 + N_4$

Absorption: $l_\mu^{cc} = \bar{l} \gamma_\mu (1 - \gamma_5) \nu_l \quad j_{cc}^\mu = \bar{\Psi}_p \left(\gamma^\mu (g_V - g_A \gamma_5) + F_2 \frac{i\sigma^{\mu\alpha} q_\alpha}{2M} \right) \Psi_n$

Scattering: $l_\mu^{nc} = \bar{\nu} \gamma_\mu (1 - \gamma_5) \nu \quad j_{nc}^\mu = \bar{\Psi}_i \left(\gamma^\mu (C_V^i - C_A^i \gamma_5) + F_2^i \frac{i\sigma^{\mu\alpha} q_\alpha}{2M} \right) \Psi_i$

Rate: $\frac{d\Gamma(E_1)}{dE_3 d\mu_{13}} = \frac{G_F^2}{32\pi^2} \frac{p_3}{E_1} (1 - f_3(E_3)) L_{\mu\nu} \mathcal{S}^{\mu\nu}(q_0, q)$

Dynamic structure function: $\mathcal{S}^{\mu\nu}(q_0, q) = \frac{-2 \text{Im } \Pi^{\mu\nu}(q_0, q)}{1 - \exp(-(q_0 + \Delta\mu)/T)}$

Current-current correlations functions: $\Pi^{\mu\nu}(q_0, q) = -i \int dt d^3x \theta(t) e^{i(q_0 t - \vec{q} \cdot \vec{x})} \langle |[j_\mu(\vec{x}, t), j_\nu(\vec{0}, 0)]| \rangle$

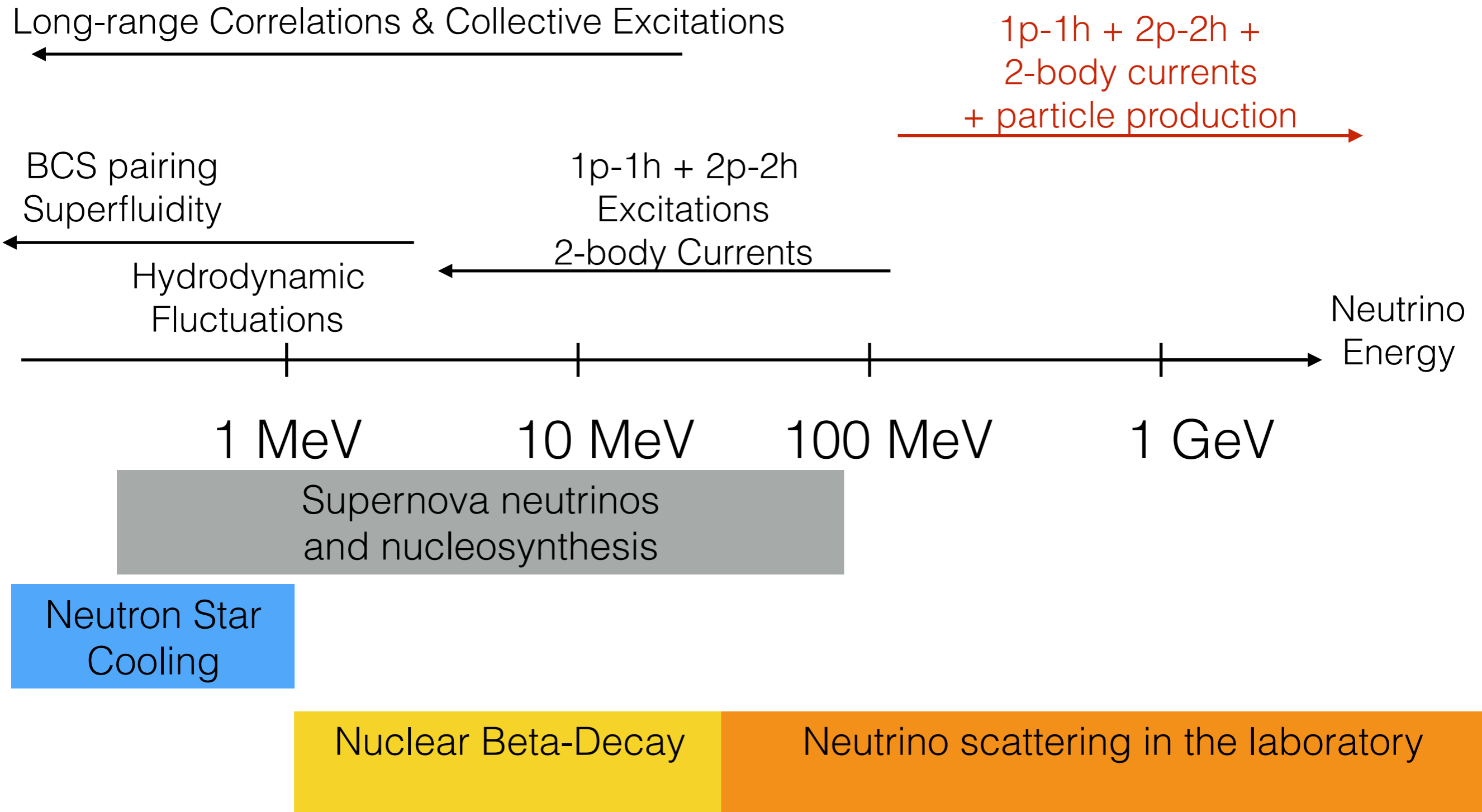
difficult to calculate in general due to the non-perturbative nature of strong interactions.

Sawyer (1970s), Iwamoto & Pethick (1980s),

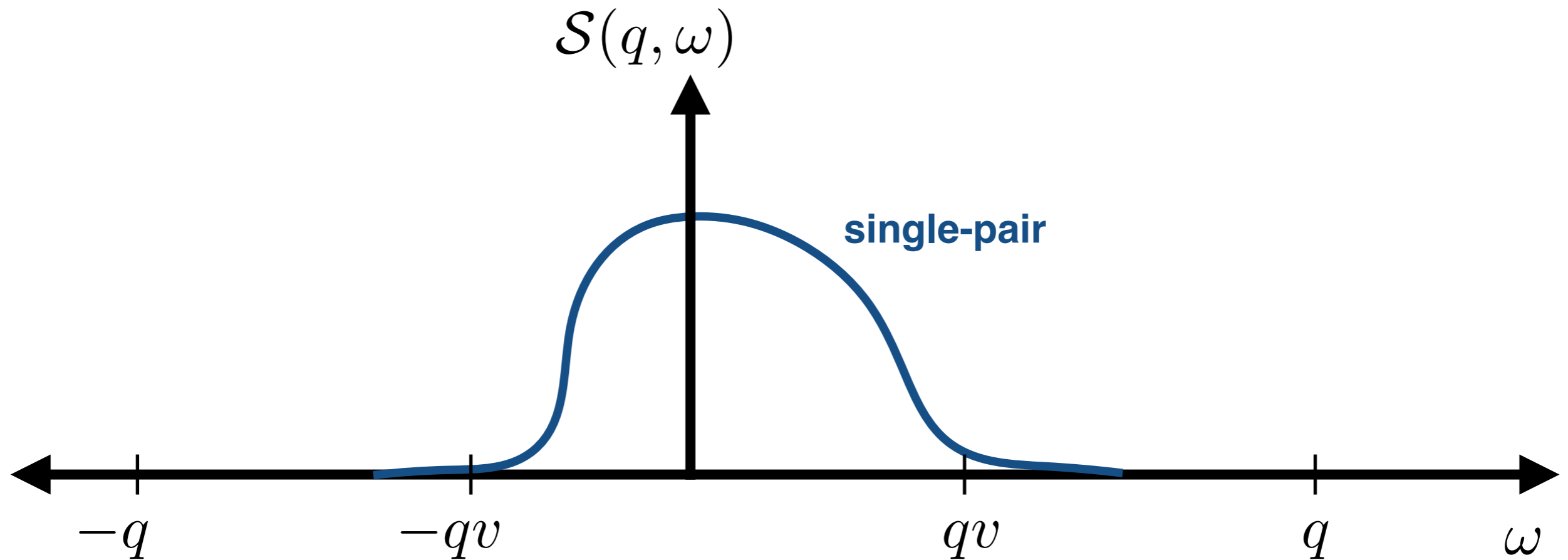
Burrows & Sawyer, Horowitz & Wehrberger, Raffelt et al., Reddy et al. (1990s),

Benhar, Carlson, Gandolfi, Horowitz, Lavato, Pethick, Reddy, Roberts, Schwenk, Shen, and others (2000s)

Correlations in Neutrino Interactions in Nuclear Matter & Nuclei



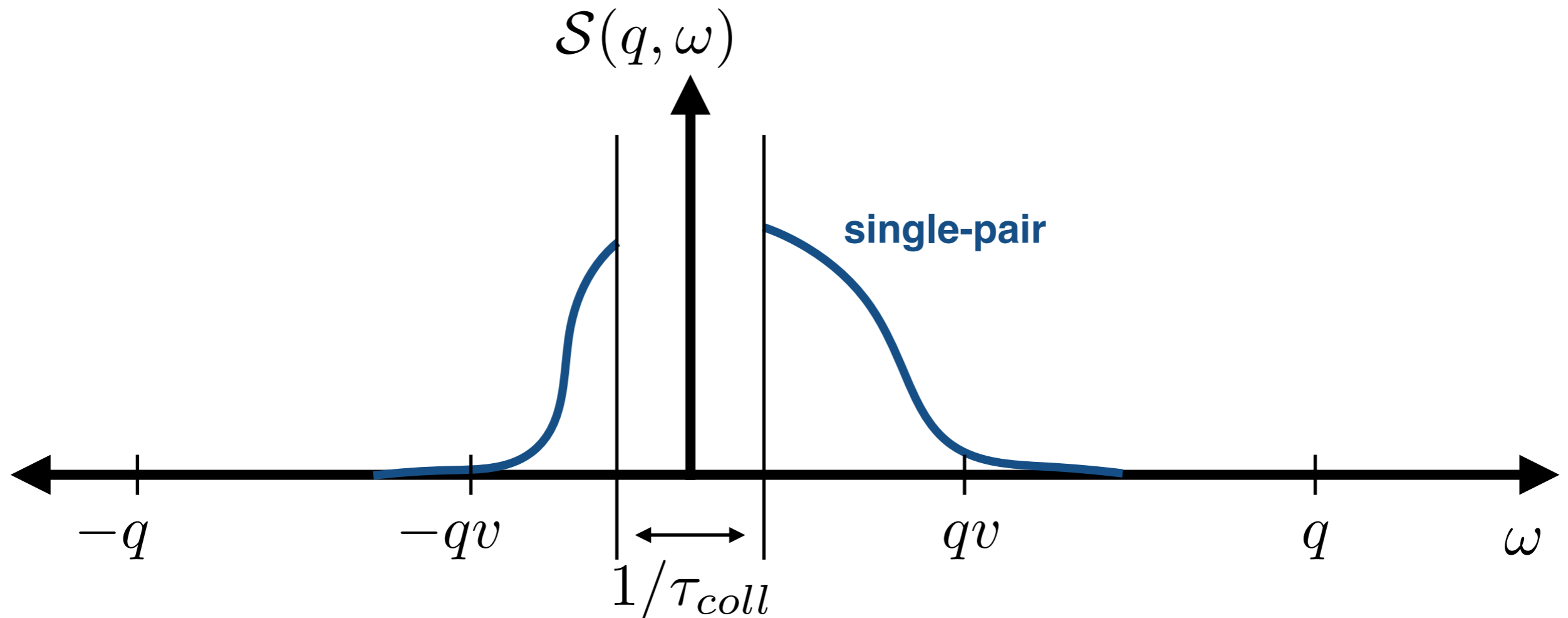
General Structure of the Dynamic Response



In hot and dense nuclear matter single-pair, multi-particle and collective modes all contribute to low energy response.

- At small ω response is governed by hydrodynamic.
- Single-pair response dominates for $|\omega\tau_{\text{coll}}| > 1$ and $|\omega| < qv$.
- Multi-particle response dominates for $|\omega| > qv$.
- Collective modes arise due to phase transitions or repulsive interactions.

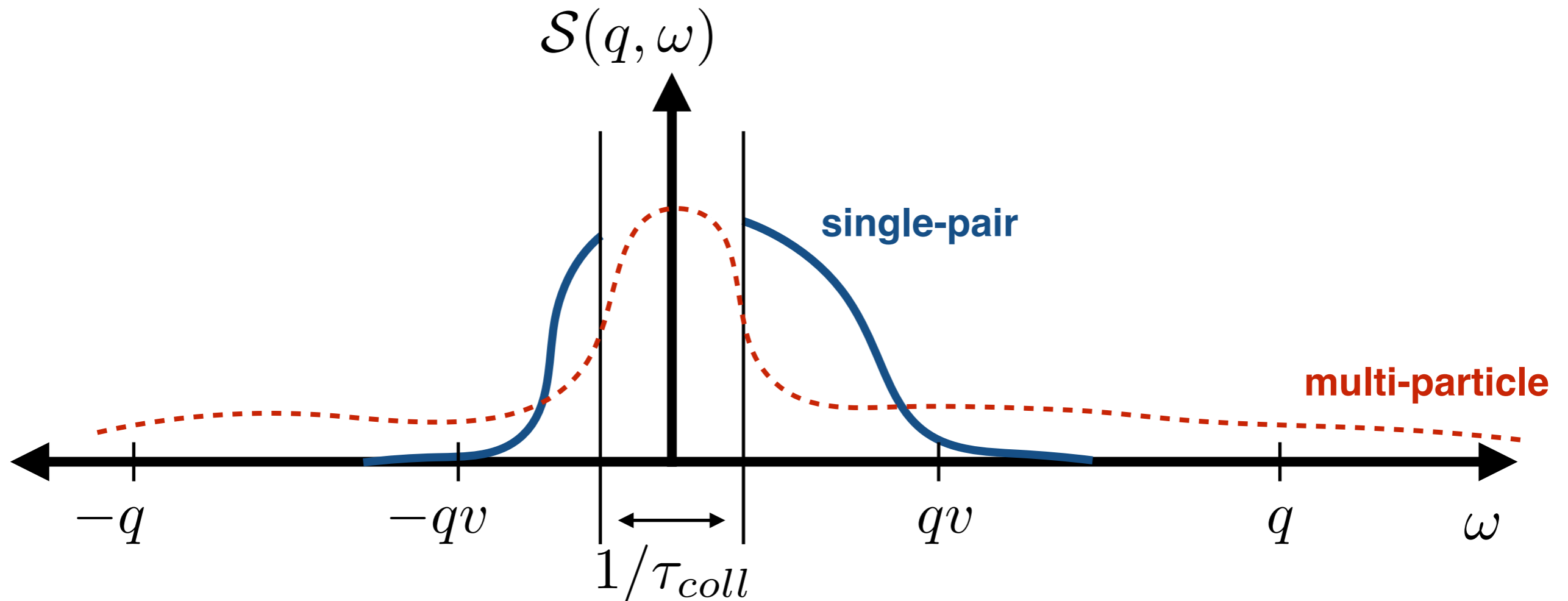
General Structure of the Dynamic Response



In hot and dense nuclear matter single-pair, multi-particle and collective modes all contribute to low energy response.

- At small ω response is governed by hydrodynamic.
- Single-pair response dominates for $|\omega\tau_{coll}| > 1$ and $|\omega| < qv$.
- Multi-particle response dominates for $|\omega| > qv$.
- Collective modes arise due to phase transitions or repulsive interactions.

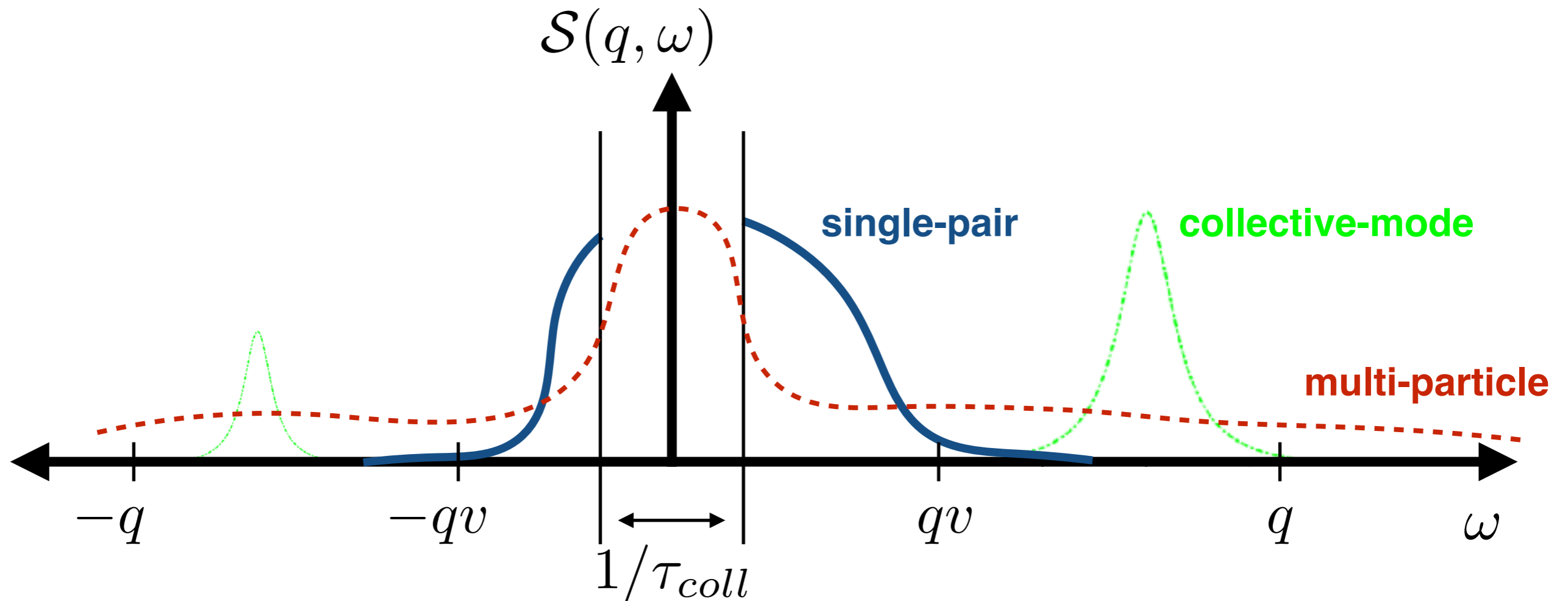
General Structure of the Dynamic Response



In hot and dense nuclear matter single-pair, multi-particle and collective modes all contribute to low energy response.

- At small ω response is governed by hydrodynamic.
- Single-pair response dominates for $|\omega\tau_{coll}| > 1$ and $|\omega| < qv$.
- Multi-particle response dominates for $|\omega| > qv$.
- Collective modes arise due to phase transitions or repulsive interactions.

General Structure of the Dynamic Response



In hot and dense nuclear matter single-pair, multi-particle and collective modes all contribute to low energy response.

- At small ω response is governed by hydrodynamic.
- Single-pair response dominates for $|\omega\tau_{coll}| > 1$ and $|\omega| < qv$.
- Multi-particle response dominates for $|\omega| > qv$.
- Collective modes arise due to phase transitions or repulsive interactions.

Linear Response

Perturbation:

$$\mathcal{H}_{int} = \int d^3x \mathcal{O}(x) \phi_{ext}(x, t)$$

Response:

$$\delta\rho(\vec{q}, \omega) = \Pi^R(\vec{q}, \omega) \phi_{ext}(\vec{q}, \omega)$$

Response function:

Polarization function

or Generalized Susceptibility

$$\Pi^R(\vec{q}, \omega) = \frac{-i}{\hbar} \int dt e^{i\omega t} \theta(t) \langle [\mathcal{O}(-\vec{q}, t), \mathcal{O}(\vec{q}, 0)] \rangle$$

Response to static and uniform perturbations is related to thermodynamic derivatives.

$$\phi_{ext}(\vec{q} \rightarrow 0, \omega = 0) = \delta\mu$$

Linear Response

Perturbation:

$$\mathcal{H}_{int} = \int d^3x \mathcal{O}(x) \phi_{ext}(x, t)$$

Response:

$$\delta\rho(\vec{q}, \omega) = \Pi^R(\vec{q}, \omega) \phi_{ext}(\vec{q}, \omega)$$

Response function:

$$\Pi^R(\vec{q}, \omega) = \frac{-i}{\hbar} \int dt e^{i\omega t} \theta(t) \langle [\mathcal{O}(-\vec{q}, t), \mathcal{O}(\vec{q}, 0)] \rangle$$

Polarization function

or Generalized Susceptibility

Response to static and uniform perturbations is related to thermodynamic derivatives.

$$\phi_{ext}(\vec{q} \rightarrow 0, \omega = 0) = \delta\mu$$

perturbation can be viewed as a change in the chemical potential 

Linear Response

Perturbation:

$$\mathcal{H}_{int} = \int d^3x \mathcal{O}(x) \phi_{ext}(x, t)$$

Response:

$$\delta\rho(\vec{q}, \omega) = \Pi^R(\vec{q}, \omega) \phi_{ext}(\vec{q}, \omega)$$

Response function:

$$\Pi^R(\vec{q}, \omega) = \frac{-i}{\hbar} \int dt e^{i\omega t} \theta(t) \langle [\mathcal{O}(-\vec{q}, t), \mathcal{O}(\vec{q}, 0)] \rangle$$

Polarization function

or Generalized Susceptibility

Response to static and uniform perturbations is related to thermodynamic derivatives.

$$\phi_{ext}(\vec{q} \rightarrow 0, \omega = 0) = \delta\mu$$

perturbation can be viewed as a change in the chemical potential \uparrow

Compressibility sum-rule:

$$\Pi^R(0, 0) = \left(\frac{\partial n}{\partial \mu} \right)_T \quad \text{where } n = \langle \mathcal{O}(0, 0) \rangle \quad \text{is the associated density.}$$

Dynamic Structure Factor

A simpler correlation function

$$\mathcal{S}(\vec{q}, \omega) = \int dt e^{i\omega t} \langle \mathcal{O}(-\vec{q}, t) \mathcal{O}(\vec{q}, 0) \rangle$$
$$= 2\pi\hbar \sum_{m,n} \frac{e^{\beta K_n}}{\mathcal{Z}} |\langle n | \mathcal{O}_q | m \rangle|^2 \delta(K_n - K_m - \hbar\omega)$$

where K_n are eigenvalues of $K = \mathcal{H} - \mu N$ (grand canonical Hamiltonian)

Fluctuation-dissipation theorem:

$$\mathcal{S}(\vec{q}, \omega) = \frac{-2\hbar \operatorname{Im} \Pi^R(\vec{q}, \omega)}{1 - e^{-\beta\hbar\omega}}$$

The dynamic structure factor incorporates all of the many-body effects into the neutrino scattering and absorption rates.

Sum Rules

Static structure factor: $\mathcal{S}_q = \int_{-\infty}^{\infty} \frac{d\omega'}{2\pi} \mathcal{S}(q, \omega')$

F-sum rule: $\int_{-\infty}^{\infty} d\omega' \omega' \text{Im} \Pi^R(q, \omega') = \langle [[\mathcal{H}, \mathcal{O}_q], \mathcal{O}_q] \rangle$

Compressibility sum-rule: $-\int_{-\infty}^{\infty} \frac{d\omega'}{\pi} \frac{\text{Im} \Pi^R(0, \omega')}{\omega'} = \text{Re} \Pi^R(0, 0) = \left(\frac{\partial n}{\partial \mu} \right)_T$

At $T=0$:

$$\int_{-\infty}^{\infty} \frac{d\omega'}{2\pi} \frac{(1 - e^{-\beta \hbar \omega'}) \mathcal{S}(q \rightarrow 0, \omega')}{\hbar \omega'} = \int_0^{\infty} \frac{d\omega'}{2\pi} \frac{\mathcal{S}(q \rightarrow 0, \omega')}{\hbar \omega'} = \left(\frac{\partial n}{\partial \mu} \right)_{T=0}$$

At high temperature: $(1 - e^{-\beta \hbar \omega'}) \simeq \beta \hbar \omega'$

$$\mathcal{S}_{q=0} = \text{lt}_{q \rightarrow 0} \int_{-\infty}^{\infty} d\omega' \mathcal{S}(q, \omega) = T \left(\frac{\partial n}{\partial \mu} \right)_T$$

Neutrino-nucleon scattering

Nucleon currents simplify
in the non-relativistic limit:

$$j_{nc}^\mu = \underbrace{\Psi^\dagger \Psi}_{\text{density}} \delta_0^\mu + \underbrace{\Psi^\dagger \sigma_k \Psi}_{\text{spin-density}} \delta_k^\mu + \mathcal{O}\left[\frac{p}{M}\right]$$

$$\frac{d\Gamma(E_1)}{d\Omega dE_3} = \frac{G_F^2}{4\pi^2} E_3^2 \left[C_V^2 (1 + \cos \theta_{13}) S_\rho(\omega, q) + C_A^2 (3 - \cos \theta_{13}) S_\sigma(\omega, q) \right]$$

Neutrino-nucleon scattering

Nucleon currents simplify
in the non-relativistic limit:

$$j_{nc}^\mu = \underbrace{\Psi^\dagger \Psi}_{\text{density}} \delta_0^\mu + \underbrace{\Psi^\dagger \sigma_k \Psi}_{\text{spin-density}} \delta_k^\mu + \mathcal{O}\left[\frac{p}{M}\right]$$

density

spin-density

dynamic response
functions

$$\frac{d\Gamma(E_1)}{d\Omega dE_3} = \frac{G_F^2}{4\pi^2} E_3^2 \left[C_V^2 (1 + \cos \theta_{13}) S_\rho(\omega, q) + C_A^2 (3 - \cos \theta_{13}) S_\sigma(\omega, q) \right]$$

Neutrino-nucleon scattering

Nucleon currents simplify
in the non-relativistic limit:

$$j_{nc}^\mu = \underbrace{\Psi^\dagger \Psi}_{\text{density}} \delta_0^\mu + \underbrace{\Psi^\dagger \sigma_k \Psi}_{\text{spin-density}} \delta_k^\mu + \mathcal{O}\left[\frac{p}{M}\right]$$

dynamic response
functions

$$\frac{d\Gamma(E_1)}{d\Omega dE_3} = \frac{G_F^2}{4\pi^2} E_3^2 \left[C_V^2 (1 + \cos \theta_{13}) S_\rho(\omega, q) + C_A^2 (3 - \cos \theta_{13}) S_\sigma(\omega, q) \right]$$

Integrate over the
final neutrino energy:

$$\frac{d\Gamma(E_1)}{dq} = \frac{G_F^2}{\pi} q \left(C_V^2 I_\rho(q) + C_A^2 I_\sigma(q) \right)$$

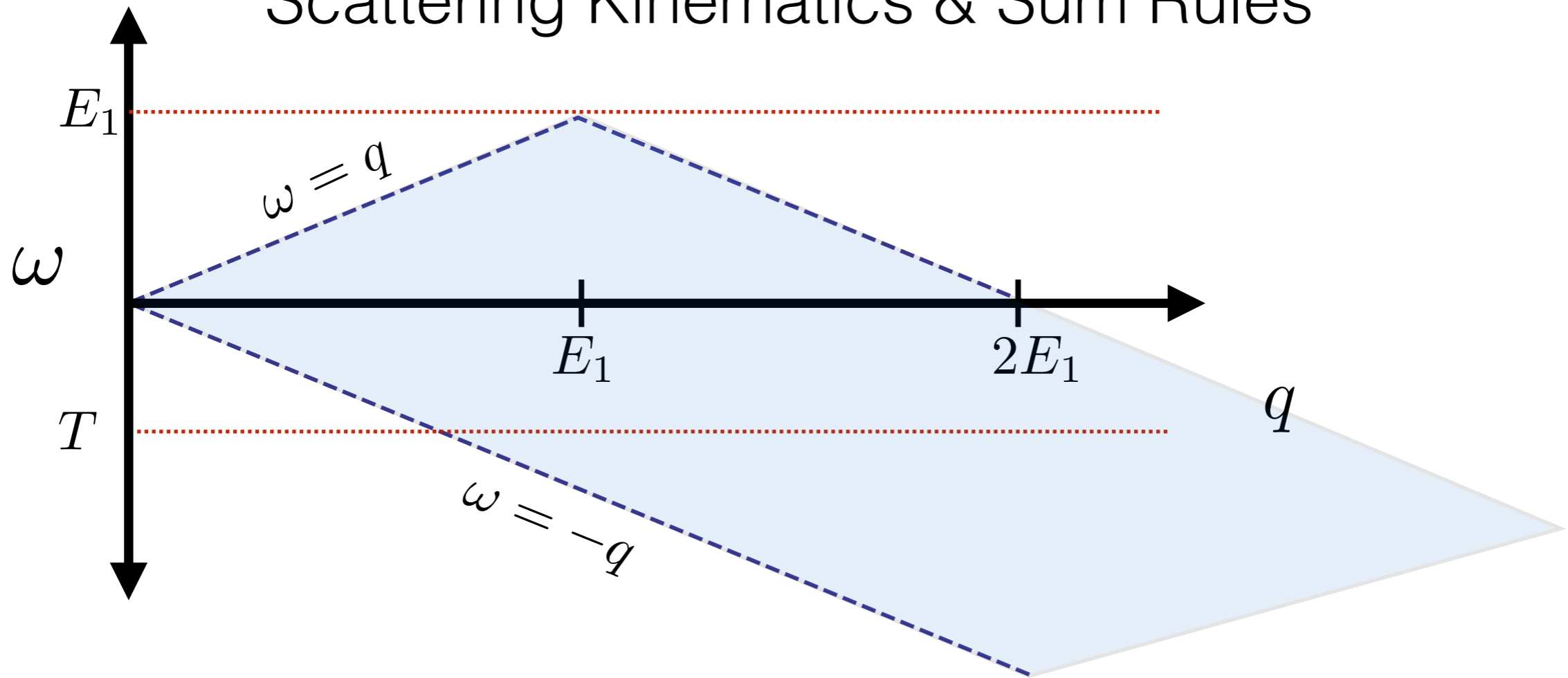
The “static”
response
functions are :

$$I_\rho(q) = \tilde{S}_\rho(q) \left(1 - \frac{q^2}{4E_1^2} - \frac{\langle \omega_\rho(q) \rangle}{E_1} + \frac{\langle \omega_\rho^2(q) \rangle}{4E_1^2} \right)$$

$$I_\sigma(q) = \tilde{S}_\sigma(q) \left(1 + \frac{q^2}{4E_1^2} - \frac{\langle \omega_\sigma(q) \rangle}{E_1} - \frac{\langle \omega_\sigma^2(q) \rangle}{4E_1^2} \right)$$

$$\tilde{S}_\alpha(q) = \int_{-q}^{\omega_{max}} d\omega S_\alpha(\omega, q) \quad \langle \omega_\alpha^n \rangle = \frac{\int_{-q}^{\omega_{max}} d\omega \omega^n S_\alpha(\omega, q)}{\tilde{S}_\alpha(q)}$$

Scattering Kinematics & Sum Rules



Neutrinos only probe the space-like region with $|\omega| < q$

In general
$$\tilde{S}_\alpha(q) = \int_{-q}^{\omega_{max}} d\omega S_\alpha(\omega, q) < S_\alpha(q) = \int_{-\infty}^{\infty} d\omega S_\alpha(\omega, q)$$

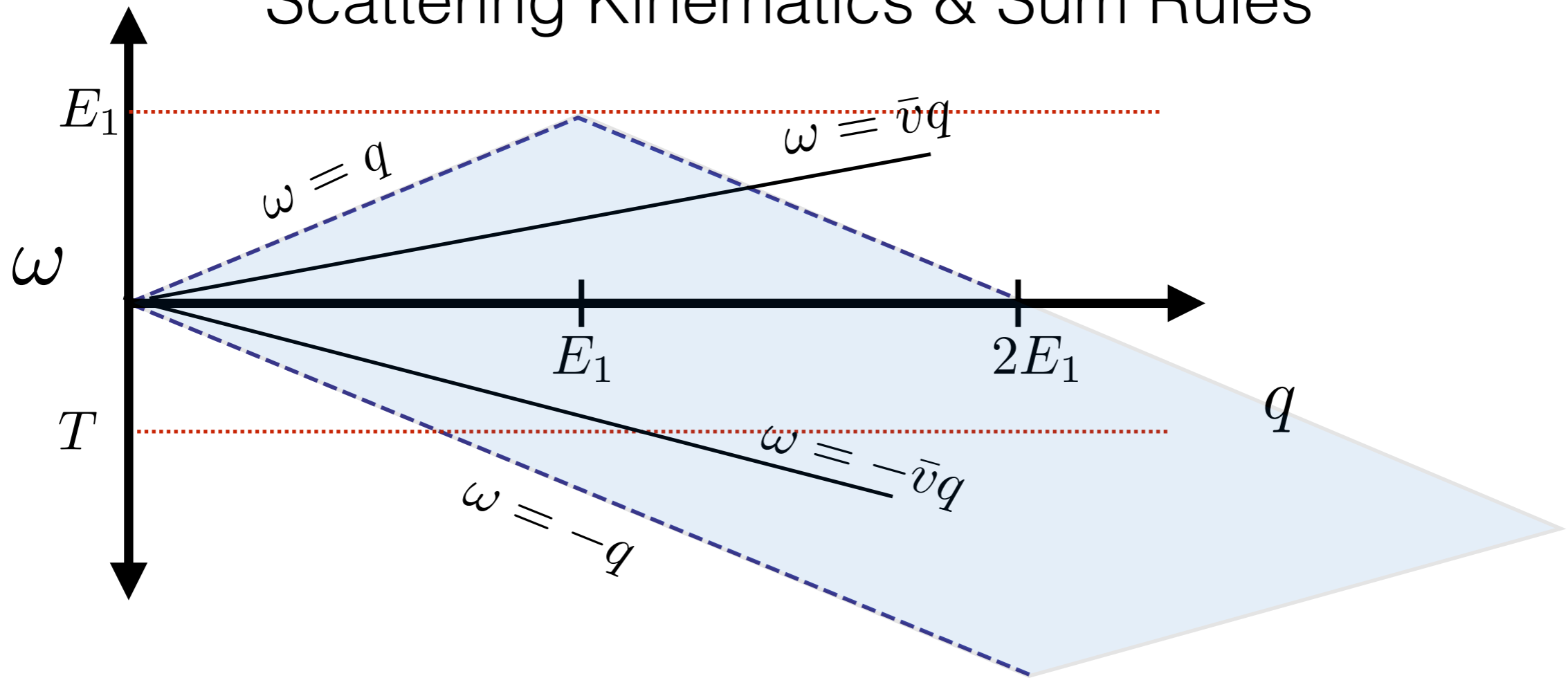
In practice for conserved currents at long-wavelengths:

$$\tilde{S}_\rho(q \rightarrow 0) = S_\rho(q \rightarrow 0)$$

$$\tilde{S}_\rho(q) \simeq S_\rho(q)$$

At high temperature recall that
$$S_\rho(q \rightarrow 0) = T \left(\frac{\partial n}{\partial \mu} \right)_T$$

Scattering Kinematics & Sum Rules



Neutrinos only probe the space-like region with $|\omega| < q$

In general
$$\tilde{S}_\alpha(q) = \int_{-q}^{\omega_{max}} d\omega S_\alpha(\omega, q) < S_\alpha(q) = \int_{-\infty}^{\infty} d\omega S_\alpha(\omega, q)$$

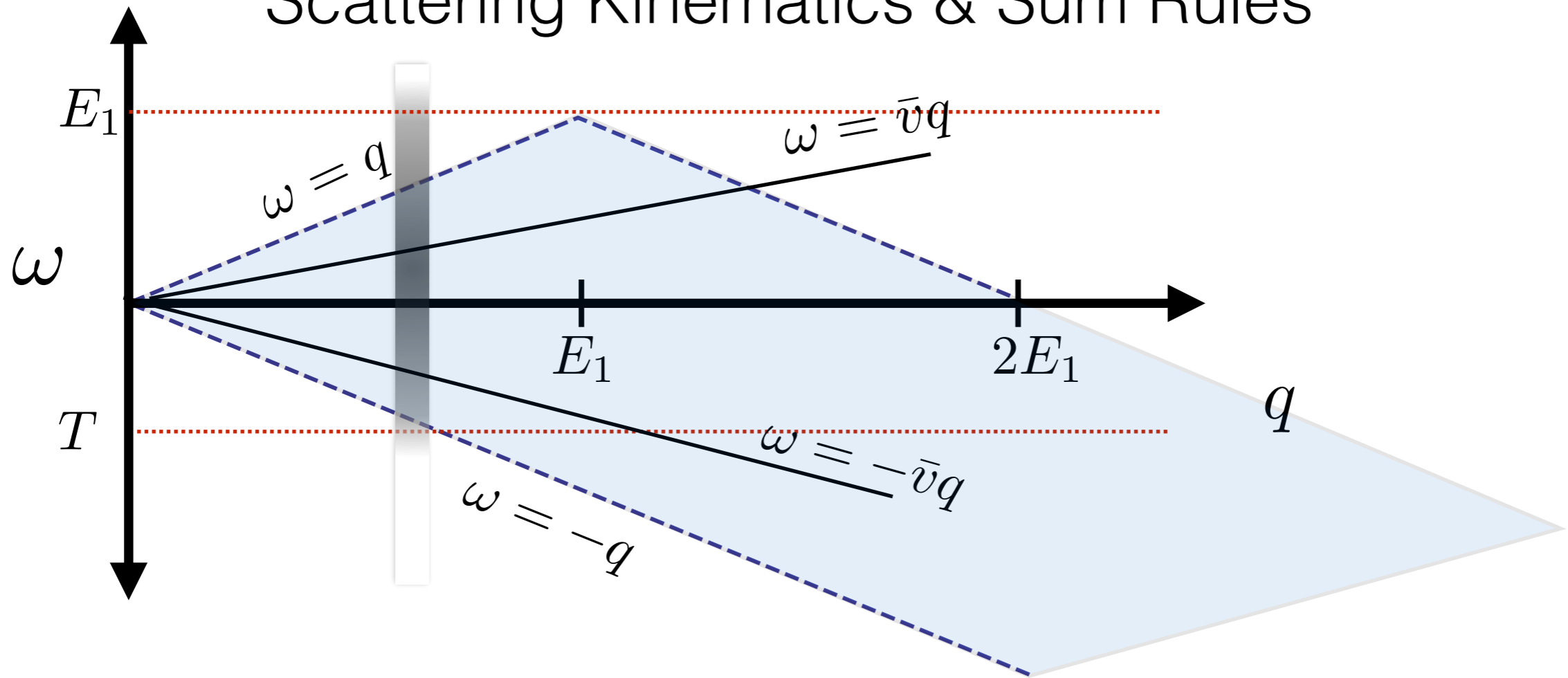
In practice for conserved currents at long-wavelengths:

$$\tilde{S}_\rho(q \rightarrow 0) = S_\rho(q \rightarrow 0)$$

$$\tilde{S}_\rho(q) \simeq S_\rho(q)$$

At high temperature recall that
$$S_\rho(q \rightarrow 0) = T \left(\frac{\partial n}{\partial \mu} \right)_T$$

Scattering Kinematics & Sum Rules



Neutrinos only probe the space-like region with $|\omega| < q$

In general
$$\tilde{S}_\alpha(q) = \int_{-q}^{\omega_{max}} d\omega S_\alpha(\omega, q) < S_\alpha(q) = \int_{-\infty}^{\infty} d\omega S_\alpha(\omega, q)$$

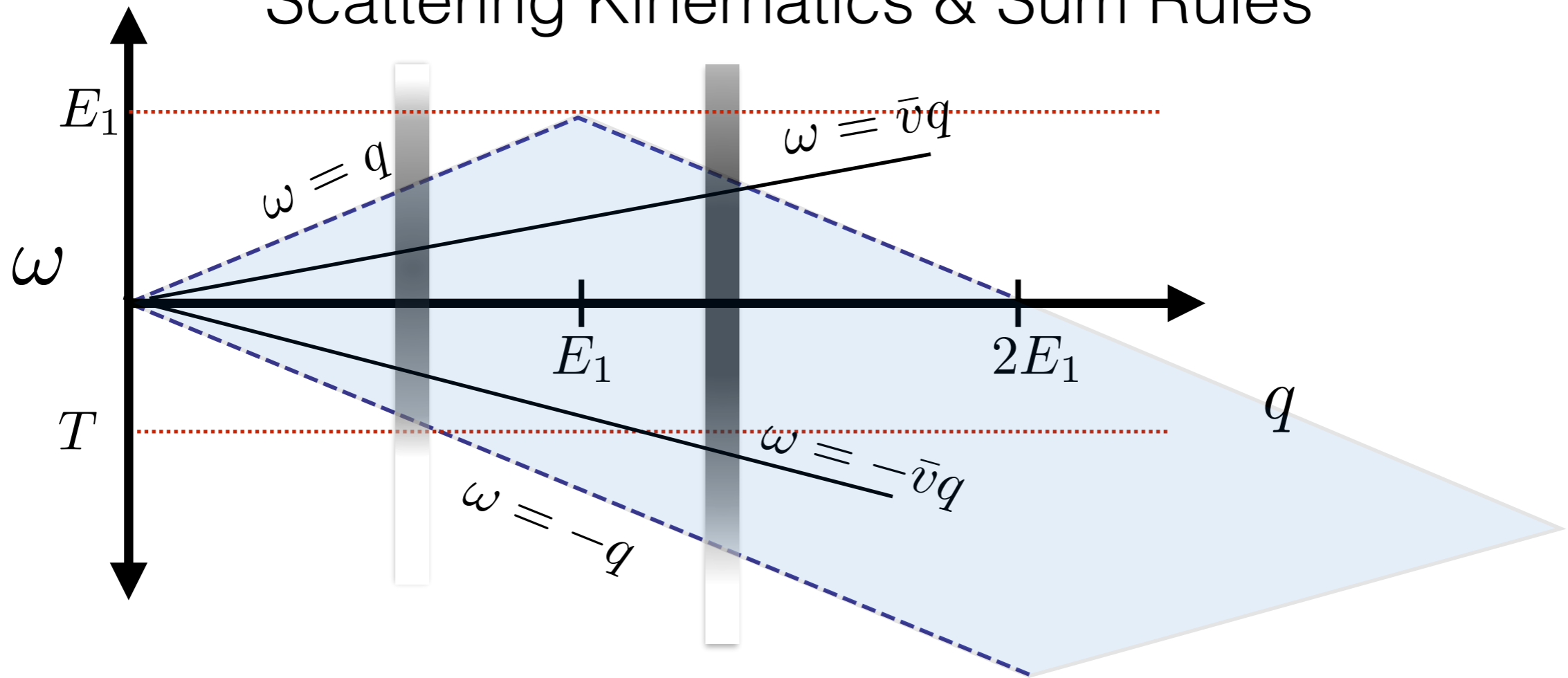
In practice for conserved currents at long-wavelengths:

$$\tilde{S}_\rho(q \rightarrow 0) = S_\rho(q \rightarrow 0)$$

$$\tilde{S}_\rho(q) \simeq S_\rho(q)$$

At high temperature recall that
$$S_\rho(q \rightarrow 0) = T \left(\frac{\partial n}{\partial \mu} \right)_T$$

Scattering Kinematics & Sum Rules



Neutrinos only probe the space-like region with $|\omega| < q$

In general
$$\tilde{S}_\alpha(q) = \int_{-q}^{\omega_{max}} d\omega S_\alpha(\omega, q) < S_\alpha(q) = \int_{-\infty}^{\infty} d\omega S_\alpha(\omega, q)$$

In practice for conserved currents at long-wavelengths:

$$\tilde{S}_\rho(q \rightarrow 0) = S_\rho(q \rightarrow 0)$$

$$\tilde{S}_\rho(q) \simeq S_\rho(q)$$

At high temperature recall that
$$S_\rho(q \rightarrow 0) = T \left(\frac{\partial n}{\partial \mu} \right)_T$$

Spin is not conserved by strong interactions

F-sum Rule:
$$F_\alpha(q) = \int d\omega \omega S_\alpha(\omega, q) = \frac{1}{2} \langle [\mathcal{O}_\alpha^\dagger, [\mathcal{O}_\alpha, H]] \rangle$$

$$F_\rho(q) = n \frac{q^2}{2m} \qquad F_\sigma(q) = C + \tilde{n} \frac{q^2}{2m}$$

- Thermodynamic derivatives may not be adequate to accurately describe the long wavelength spin response.
- Some dynamical information is needed to calculate neutrino scattering rates in the medium.

Spin is not conserved by strong interactions

F-sum Rule:
$$F_\alpha(q) = \int d\omega \omega S_\alpha(\omega, q) = \frac{1}{2} \langle [\mathcal{O}_\alpha^\dagger, [\mathcal{O}_\alpha, H]] \rangle$$

$$F_\rho(q) = n \frac{q^2}{2m} \qquad F_\sigma(q) = C + \tilde{n} \frac{q^2}{2m}$$

↑
1p-1h contribution dominates.
No time-like response.

$$\tilde{S}_\rho(q) = \int_{-q}^{\omega_{max}} d\omega S_\rho(\omega, q) \simeq S_\rho(q)$$

- Thermodynamic derivatives may not be adequate to accurately describe the long wavelength spin response.
- Some dynamical information is needed to calculate neutrino scattering rates in the medium.

Spin is not conserved by strong interactions

F-sum Rule:
$$F_\alpha(q) = \int d\omega \omega S_\alpha(\omega, q) = \frac{1}{2} \langle [\mathcal{O}_\alpha^\dagger, [\mathcal{O}_\alpha, H]] \rangle$$

$$F_\rho(q) = n \frac{q^2}{2m}$$

↑
1p-1h contribution dominates.
No time-like response.

$$F_\sigma(q) = C + \tilde{n} \frac{q^2}{2m}$$

↑
2p-2h contribution
Finite time-like response.

$$\tilde{S}_\rho(q) = \int_{-q}^{\omega_{max}} d\omega S_\rho(\omega, q) \simeq S_\rho(q)$$

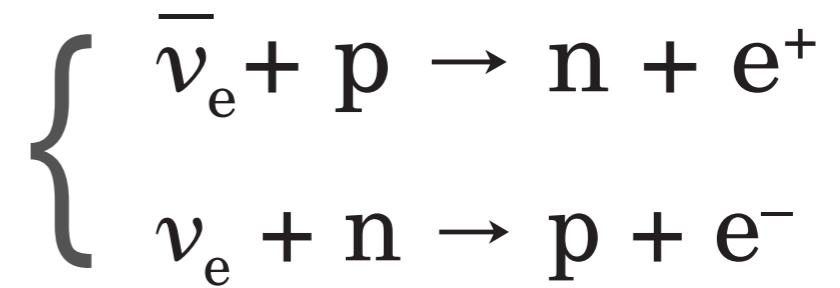
$$\tilde{S}_\sigma(q) = \int_{-q}^{\omega_{max}} d\omega S_\sigma(\omega, q) < S_\sigma(q)$$

- Thermodynamic derivatives may not be adequate to accurately describe the long wavelength spin response.
- Some dynamical information is needed to calculate neutrino scattering rates in the medium.

Supernova Neutrino Spectra and Nucleosynthesis

Electron and anti-electron neutrinos play a crucial role in supernova. Their energy spectrum impacts:

1. Explosion mechanism
2. Nucleosynthesis
3. Detection

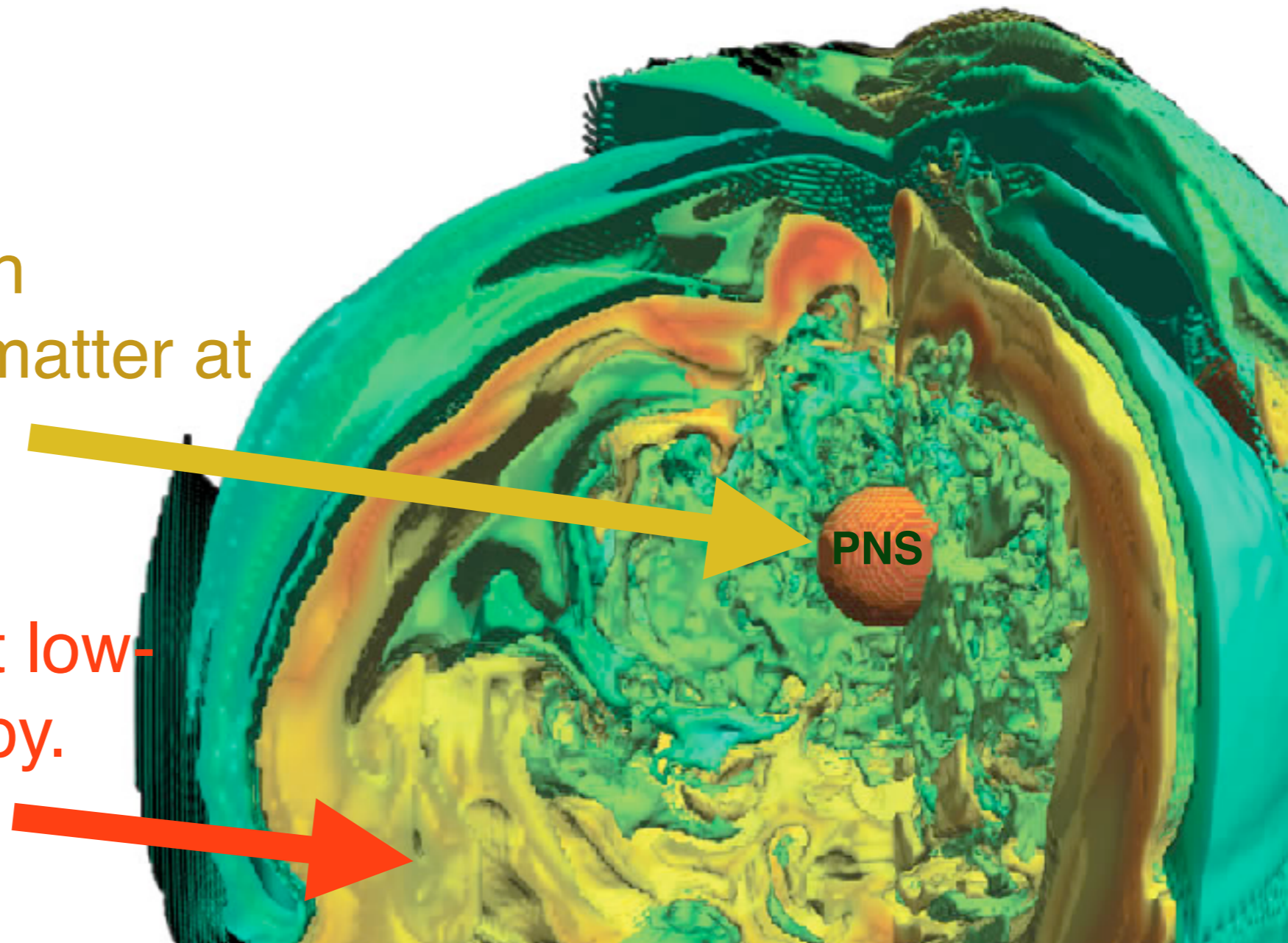


Neutrino-sphere at high density. Neutron-rich matter at moderate entropy.

$R \sim 10\text{-}20 \text{ km}$

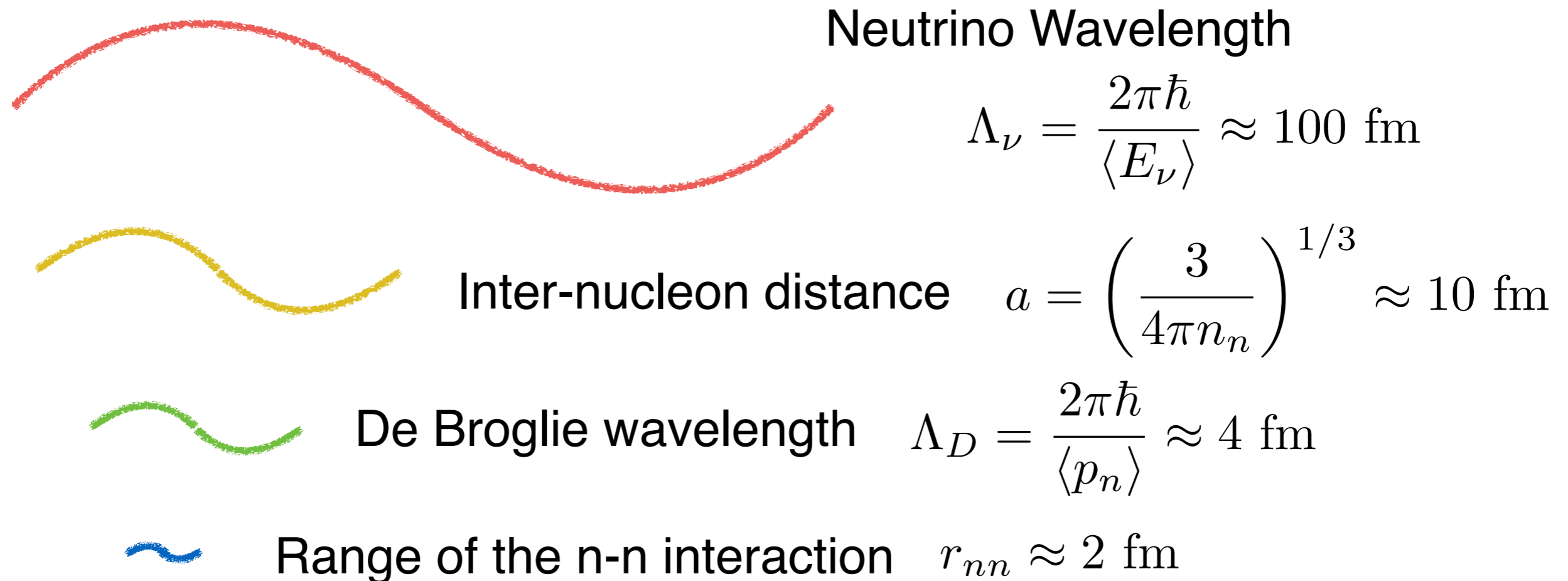
Neutrino driven wind at low-density and high entropy.

$R \sim 10^3\text{-}10^4 \text{ km}$



10^{12} g/cm^3 : Neutrino Processes in the Neutrino-sphere

Hierarchy of length scales at $T=5 \text{ MeV}$ and $\rho = 10^{12} \text{ g/cm}^3$



- Matter is dilute, but interactions are strong and non-perturbative.
- Nucleon-nucleon scattering length is large $\sim 20 \text{ fm}$.
- Small expansion parameter is the fugacity $z=e^{\mu/T}$ - virial expansion.
- Horowitz & Schwenk developed a virial EoS in this regime.

Long-wavelength Response using the Virial EoS

Assumes that scattering is nearly elastic to include all many-body correlations through the static structure factors.

$$\tilde{S}_\rho(q) = \int_{-q}^{\omega_{max}} d\omega S_\rho(\omega, q) \simeq S_\rho(q) \qquad \tilde{S}_\rho(q \rightarrow 0) = S_\rho(q \rightarrow 0)$$

Calculate the static structure factors using the compressibility or thermodynamic sum rule

$$S_\rho(q \rightarrow 0) = T \left(\frac{\partial n}{\partial \mu} \right)_T$$

Sawyer (1975, 1979)

Horowitz and Schwenk (2005), Horowitz et al. (2017)

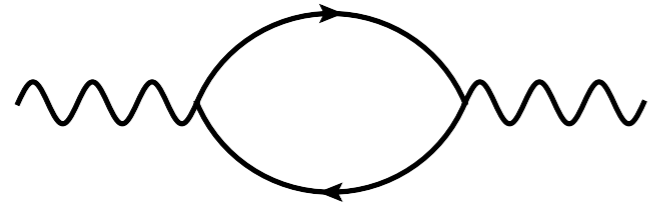
This is an excellent approximation for the density response relevant to neutral current reactions in the neutrino sphere.

The spin response and charged current reactions require some dynamical input.

Pseudo-potential for Hot & Dilute Nuclear Matter

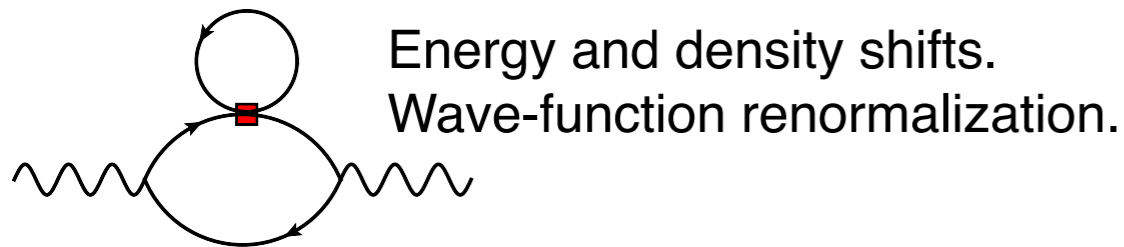
The dynamic structure factor calculable using standard diagrammatic “perturbation” theory - with a twist.

Interactions represented by a pseudo-potential: $\mathcal{V}_{ps} \propto \frac{\delta(p_{rel})}{p_{rel} M}$



Leading order diagram neglects interactions.

$$\mathcal{O}[z]$$

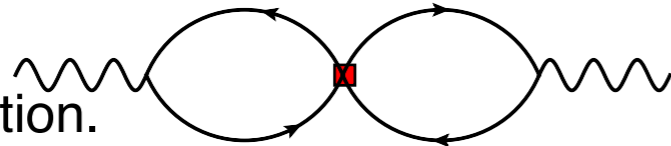


Energy and density shifts.
Wave-function renormalization.

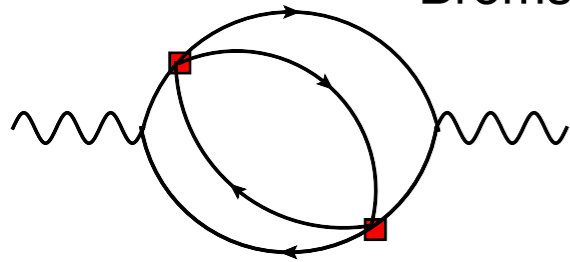
Includes interactions at leading order. Consistent with the virial expansion.

$$\mathcal{O}[z^2 \mathcal{V}_{ps}]$$

Screening.
Vertex renormalization.



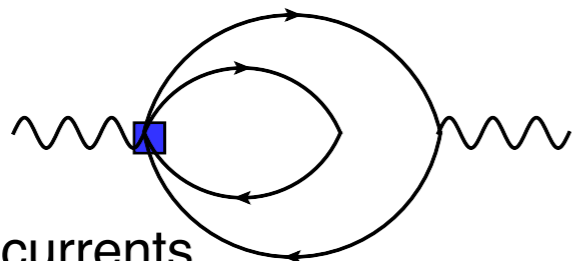
Bremsstrahlung processes



Includes 2p-2h excitations and 2-body currents. These corrections are beyond the leading order virial expansion.

$$\mathcal{O}[z^2 \mathcal{V}_{ps}^2]$$

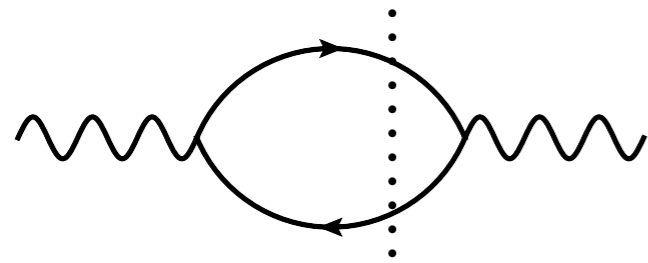
2-body or meson-exchange currents



Pseudo-potential for Hot & Dilute Nuclear Matter

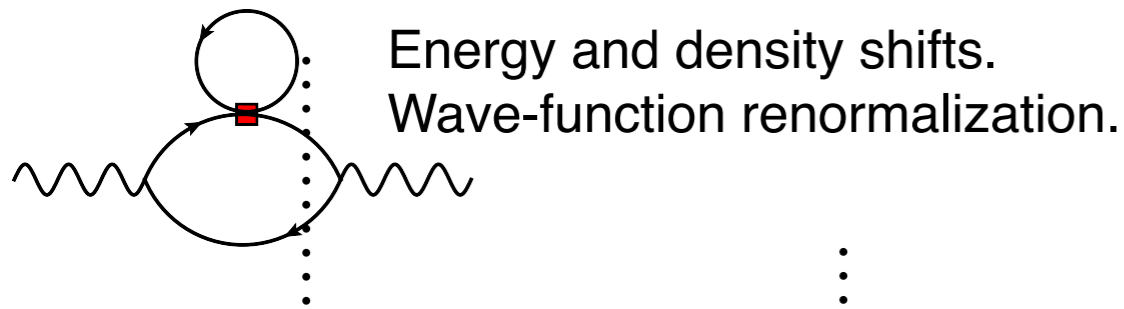
The dynamic structure factor calculable using standard diagrammatic “perturbation” theory - with a twist.

Interactions represented by a pseudo-potential: $\mathcal{V}_{ps} \propto \frac{\delta(p_{rel})}{p_{rel} M}$



Leading order diagram neglects interactions.

$$\mathcal{O}[z]$$

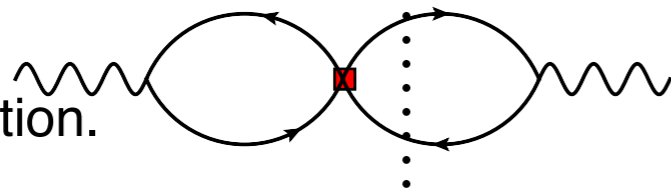


Energy and density shifts.
Wave-function renormalization.

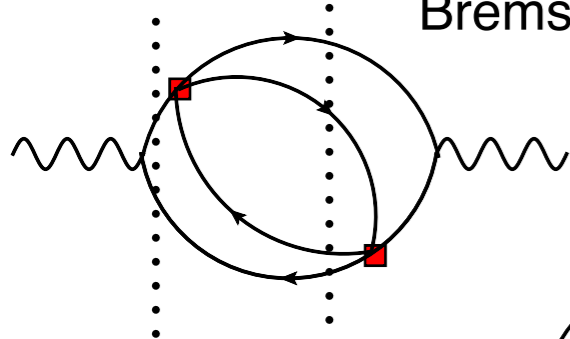
Includes interactions at leading order. Consistent with the virial expansion.

$$\mathcal{O}[z^2 \mathcal{V}_{ps}]$$

Screening.
Vertex renormalization.



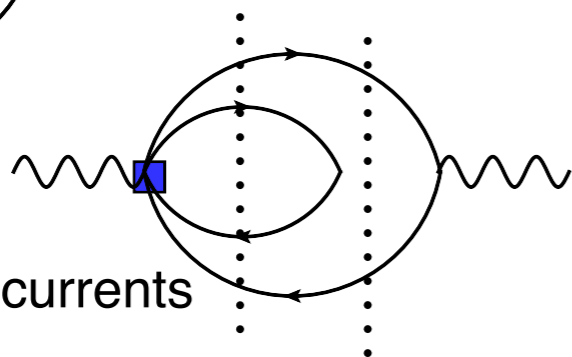
Bremsstrahlung processes



Includes 2p-2h excitations and 2-body currents. These corrections are beyond the leading order virial expansion.

$$\mathcal{O}[z^2 \mathcal{V}_{ps}^2]$$

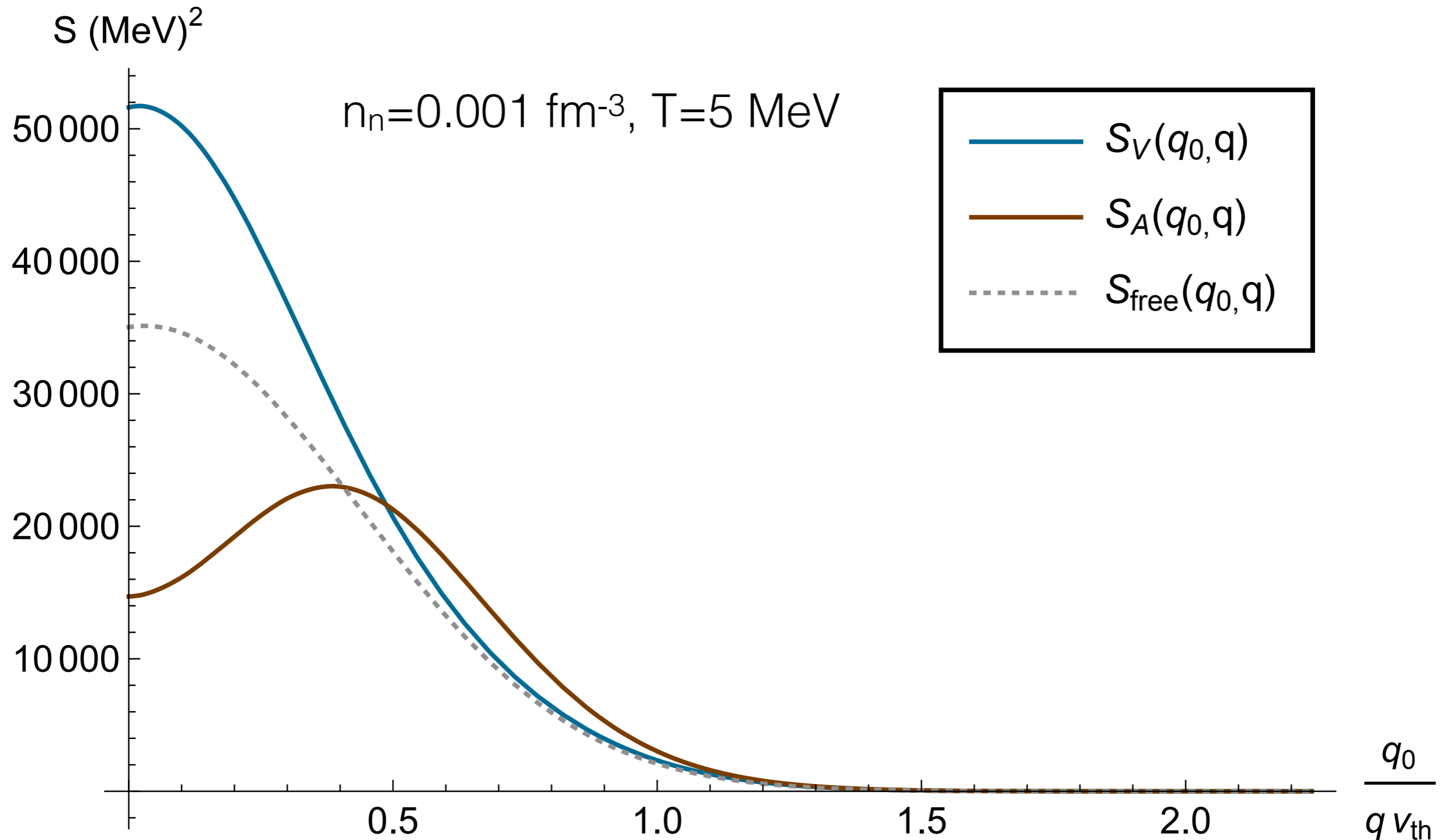
2-body or meson-exchange currents



Dynamic Structure Factor with Pseudo-potential

$$S_{\text{total}} = \text{[Diagram 1]} + \text{[Diagram 2]} + \text{[Diagram 3]}$$

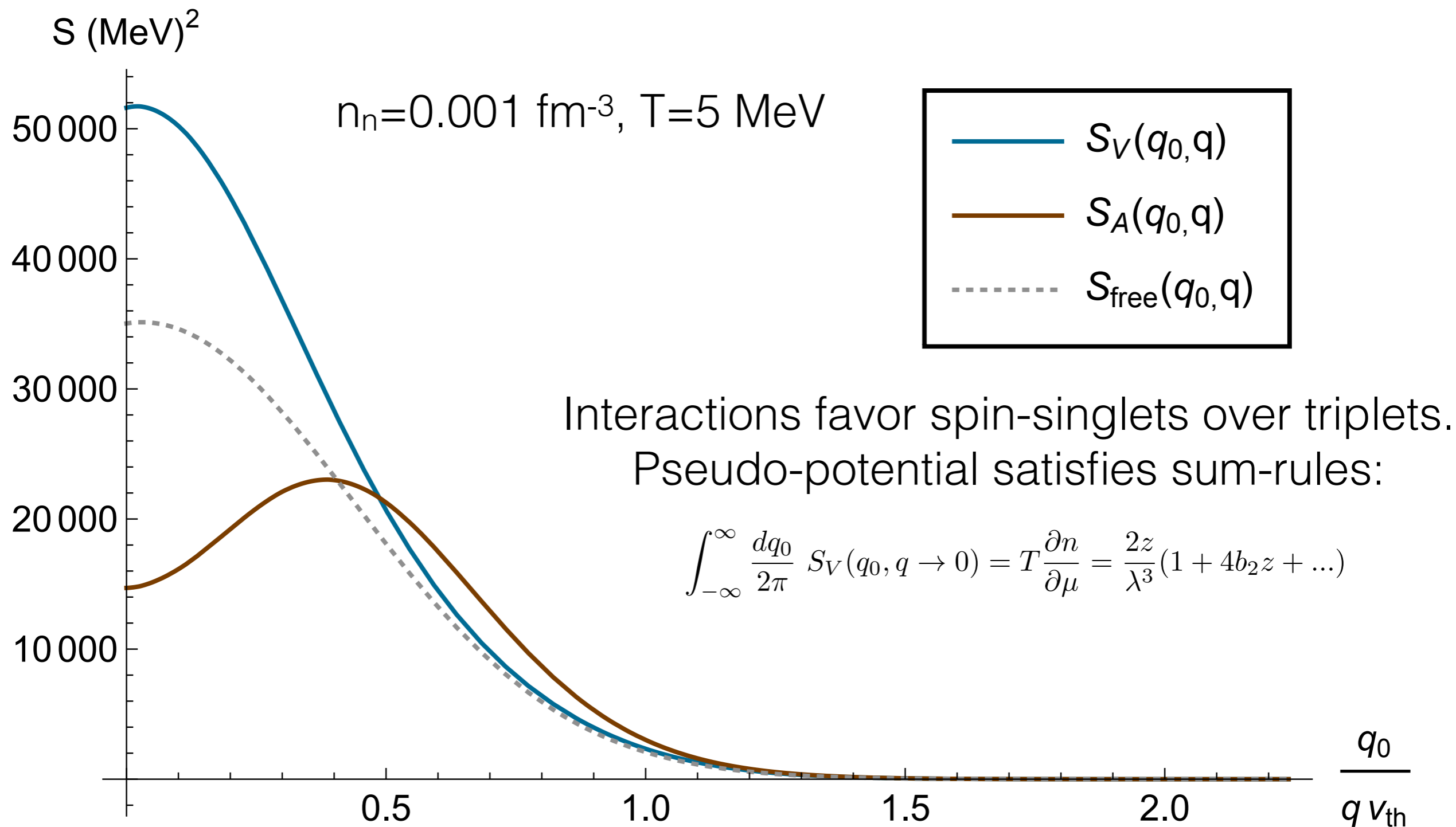
The diagrams represent Feynman diagrams for the dynamic structure factor. Diagram 1 is a bubble diagram with two wavy external lines. Diagram 2 is a bubble diagram with a self-energy loop on the top line and a wavy external line on the right. Diagram 3 is a bubble diagram with two bubbles connected by a wavy line, and wavy external lines on both ends.



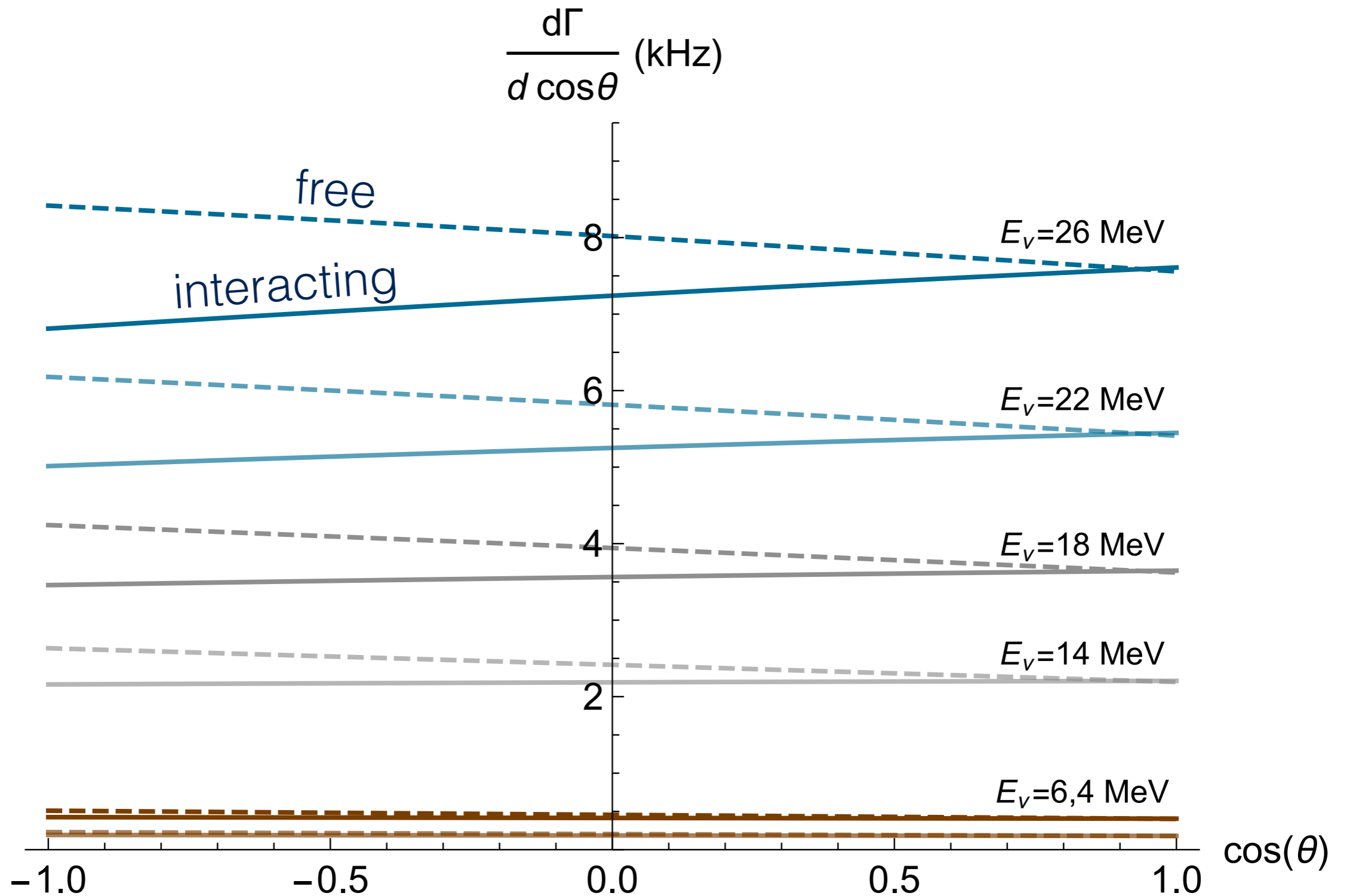
Dynamic Structure Factor with Pseudo-potential

$$S_{\text{total}} = \text{[Diagram 1]} + \text{[Diagram 2]} + \text{[Diagram 3]}$$

The diagrams represent Feynman diagrams for the dynamic structure factor. The first diagram is a bubble diagram with two wavy external lines. The second diagram is a bubble diagram with a self-energy loop on the top line and a wavy external line on the right. The third diagram is a bubble diagram with two bubbles connected by a wavy line, and wavy external lines on both ends.

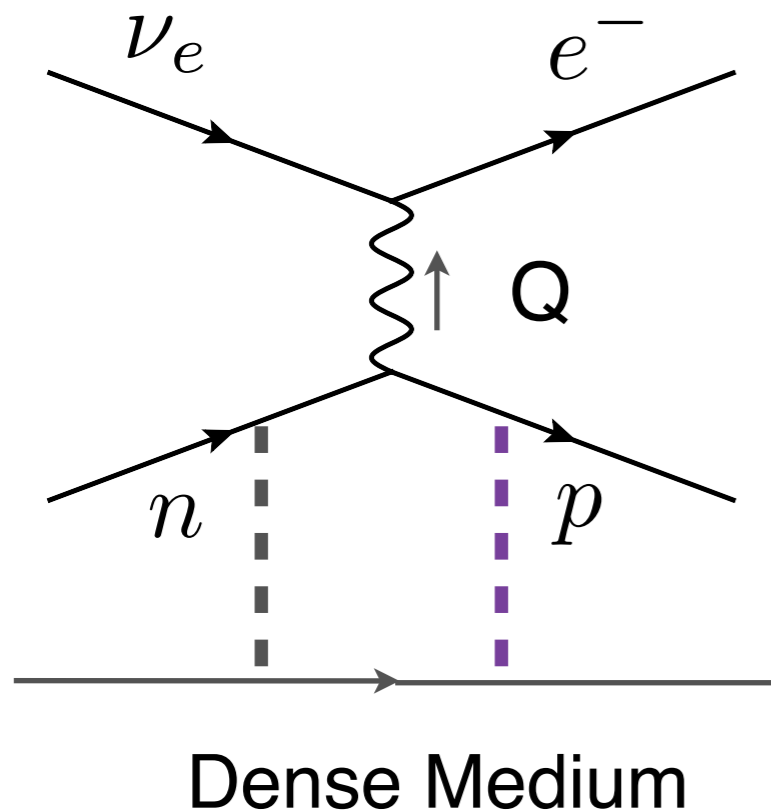


Back-scattering is suppressed



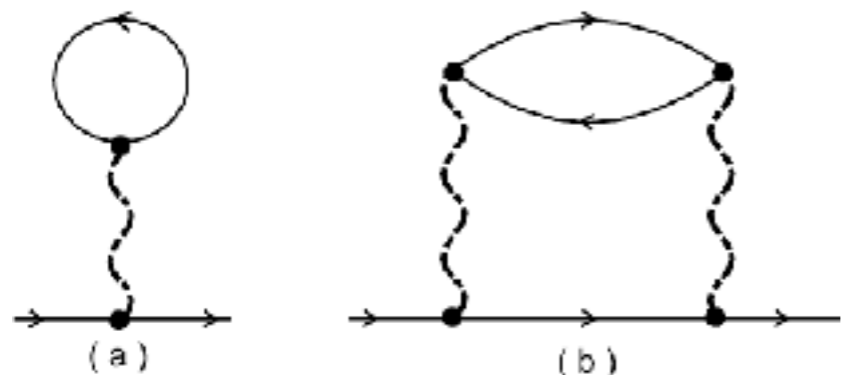
A reduced axial response implies a reduced scattering at backward angles : Important for transport and spectra.

Charged Current Reactions in Neutron-Rich Matter



Potential energy difference between neutrons and protons is large - and related to the low density symmetry energy.

The pseudo-potential is suitable to calculate the nucleon self-energy.



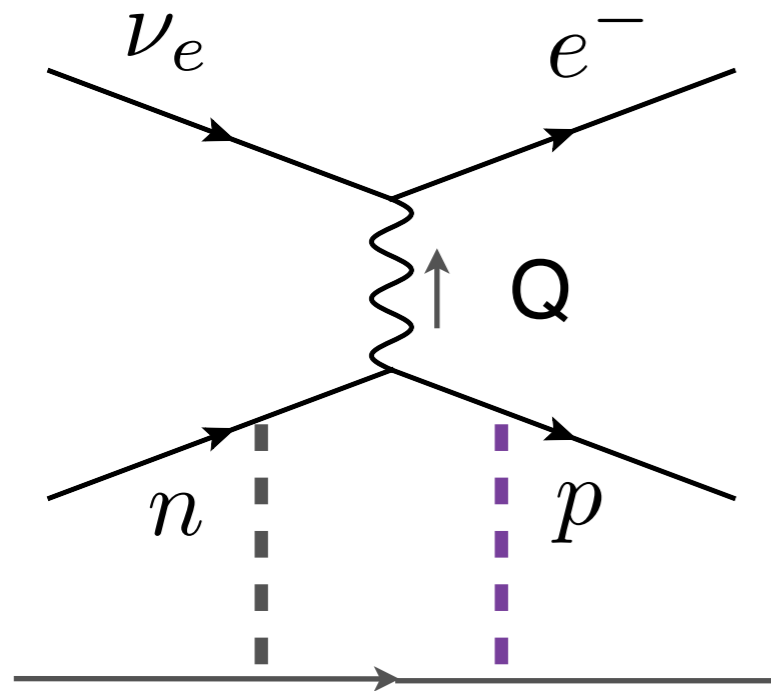
$$E_n(p) \approx m_n + \frac{p^2}{2m_n^*} + U_n + i \Gamma_n$$

$$E_p(p + q) \approx m_p + \frac{(p + q)^2}{2m_n^*} + U_p + i \Gamma_p$$

$$Q = \varepsilon_n(\vec{k}) - \varepsilon_p(\vec{k} - \vec{q})$$

$$= M_n - M_p + \Sigma_n(k) - \Sigma_n(k - q)$$

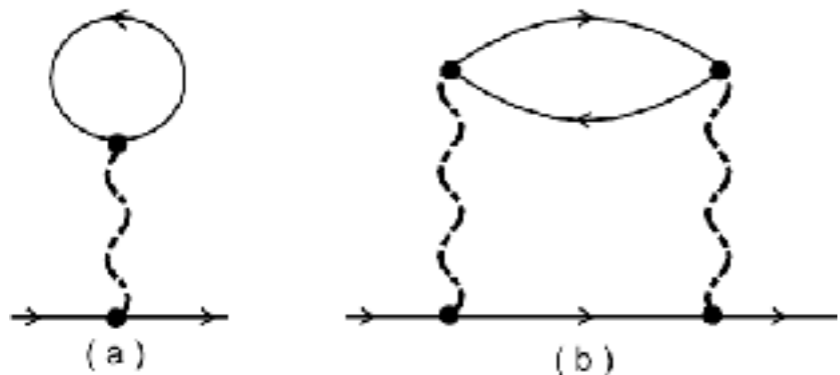
Charged Current Reactions in Neutron-Rich Matter



Potential energy difference between neutrons and protons is large - and related to the low density symmetry energy.

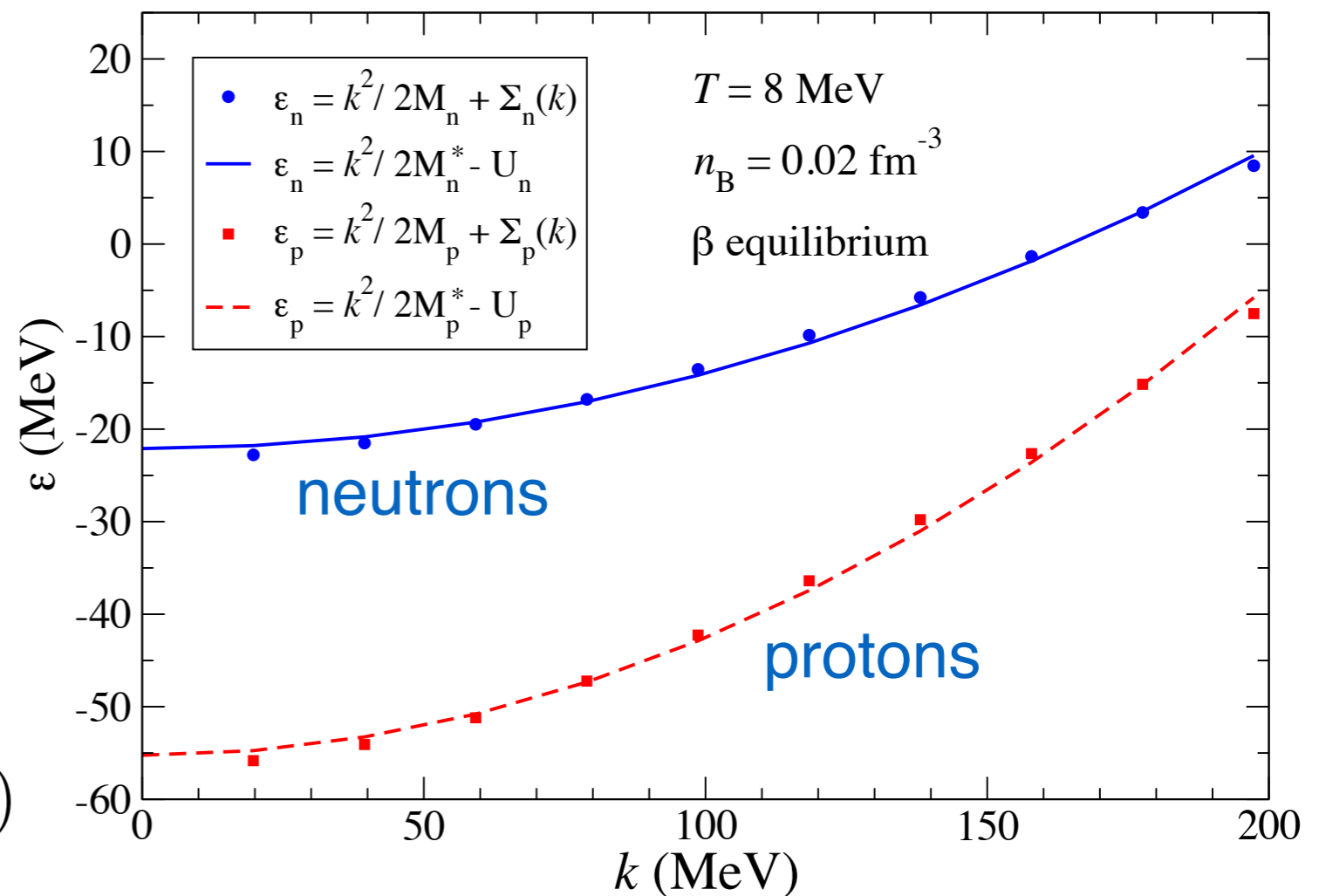
The pseudo-potential is suitable to calculate the nucleon self-energy.

Dense Medium



$$Q = \varepsilon_n(\vec{k}) - \varepsilon_p(\vec{k} - \vec{q})$$

$$= M_n - M_p + \Sigma_n(k) - \Sigma_n(k - q)$$



Mean Field & Collisional Broadening

Ansatz for the spin-isospin charge-exchange response function in hot matter:

$$S_{\sigma\tau-}(q_0, q) = \frac{1}{1 - \exp(-\beta(q_0 + \mu_n - \mu_p))} \text{Im} \left[\frac{\tilde{\Pi}(q_0, q)}{1 - V_{\sigma\tau}\tilde{\Pi}(q_0, q)} \right]$$

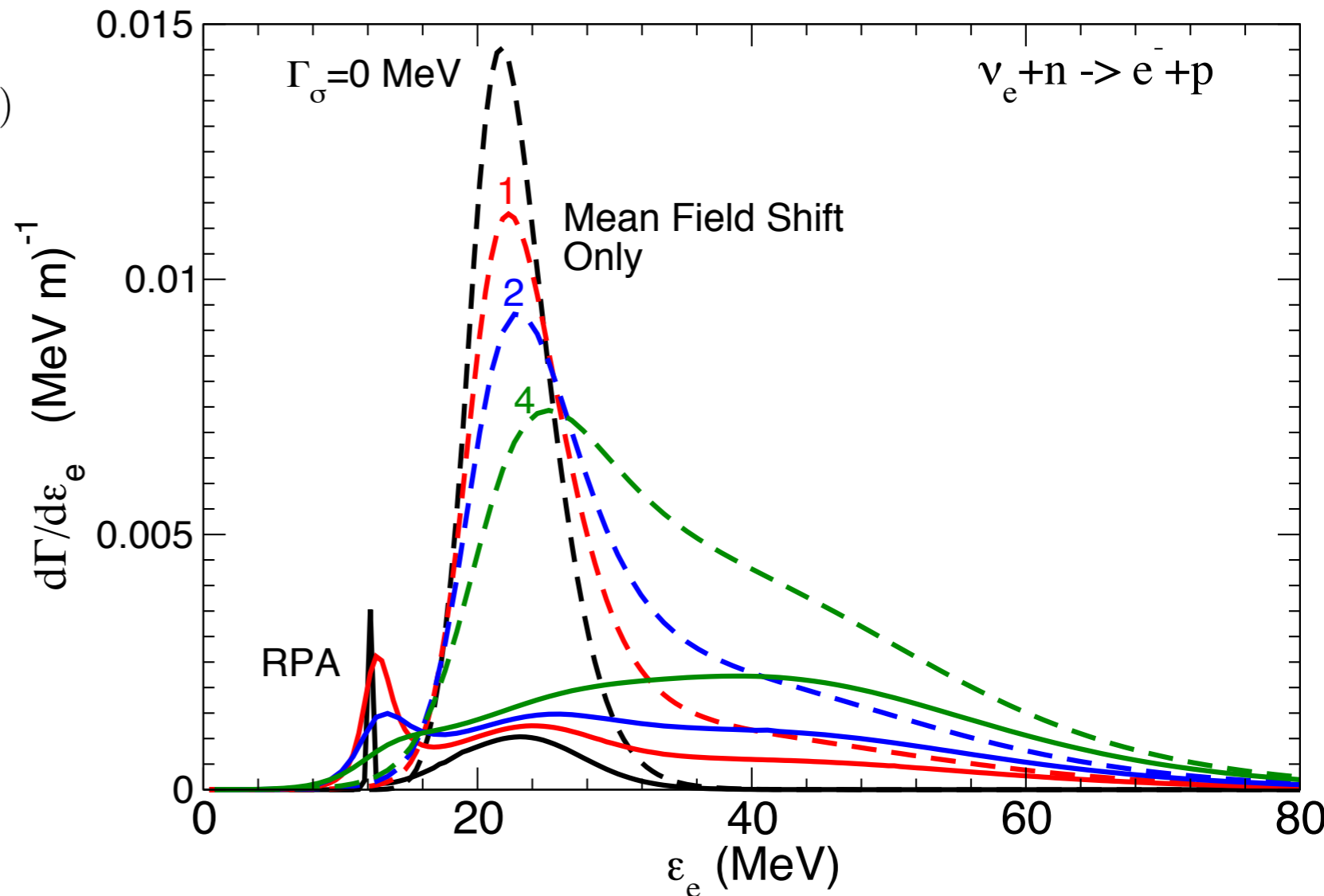
$$V_{\sigma\tau} \simeq 200 - 220 \text{ MeV/fm} \quad \text{G. Bertsch, D. Cha, and H. Toki (1984)}$$

Collisional broadening (finite lifetime) introduced in the relaxation time approximation: $\Gamma = \tau_{\sigma}^{-1}$

$$\text{Im}\tilde{\Pi}(q_0, q) = \frac{1}{\pi} \int \frac{d^3p}{(2\pi)^3} \frac{f_p(\epsilon_{p+q}) - f_n(\epsilon_p)}{\epsilon_{p+q} - \epsilon_p + \hat{\mu}} \mathcal{I}(\Gamma)$$

$$\mathcal{I}(\Gamma) = \frac{\Gamma}{(q_0 + \Delta U - (\epsilon_{p+q} - \epsilon_p))^2 + \Gamma^2}$$

Energy shifts, the Gamow-Teller resonance and collisional broadening all play a role.

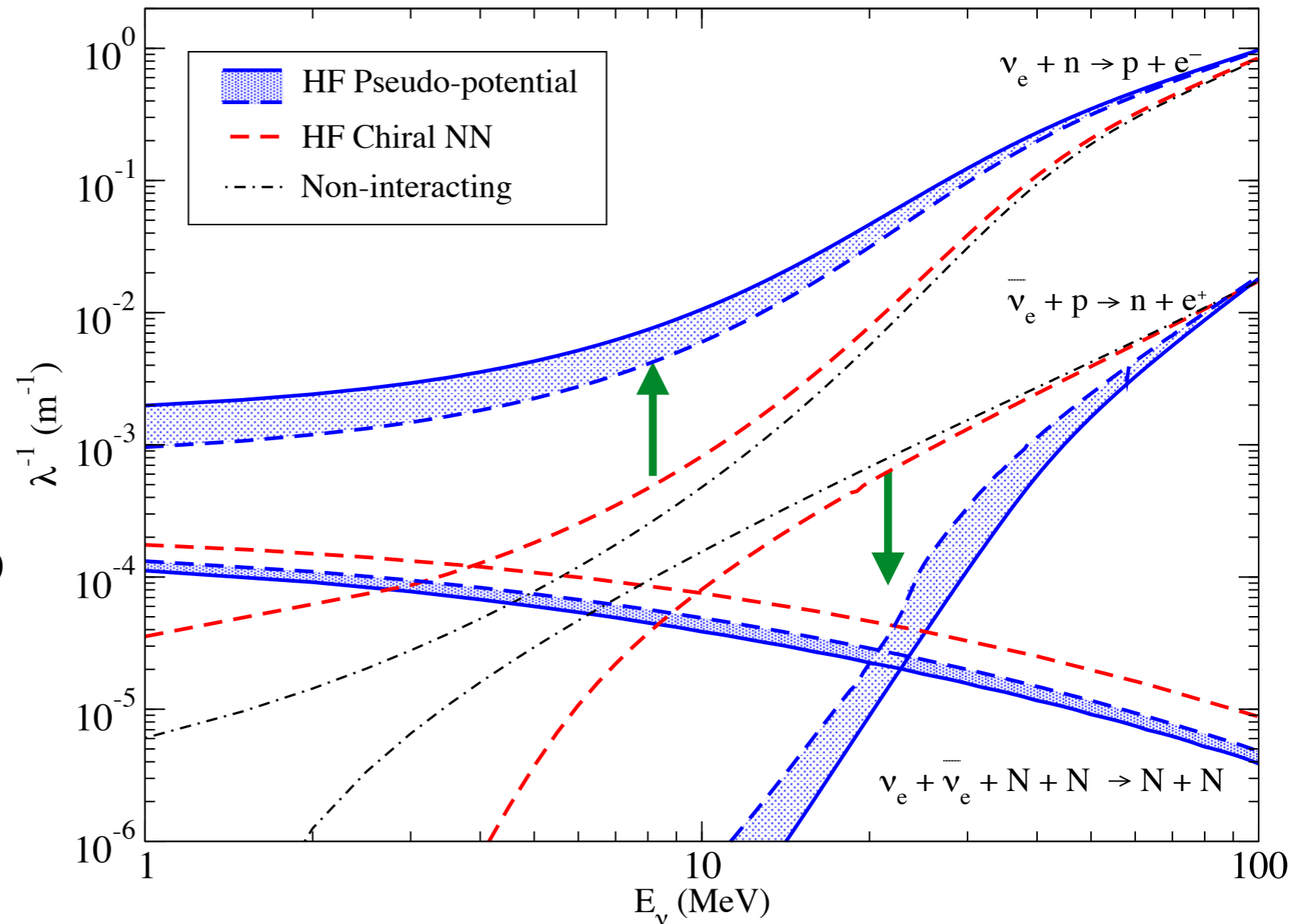


Shen, Roberts, Reddy (2013)

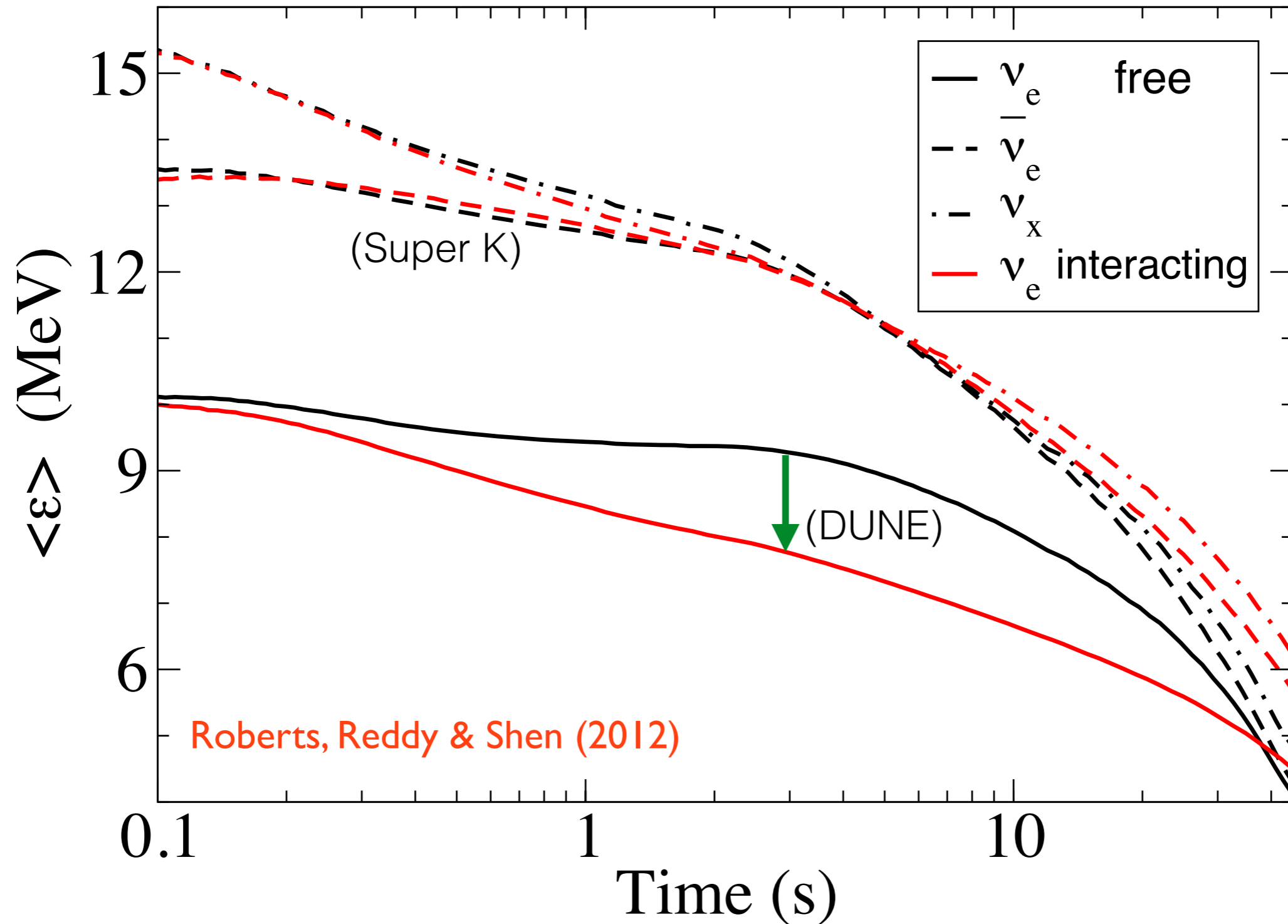
Charged Currents at Low Density with the Pseudo-potential

$$\frac{d\Gamma}{\cos\theta dE_e} = \frac{G_F^2}{2\pi} p_e E_e (1 - f_e(E_e)) \times [(1 + \cos\theta)S_\tau(q_0, q) + g_A^2(3 - \cos\theta)S_{\sigma\tau}(q_0, q)]$$

- Energy shift helps overcome electron final state blocking.
- Enhances ν_e absorption
- Larger energy needed to produce neutrons suppresses anti- ν_e absorption.



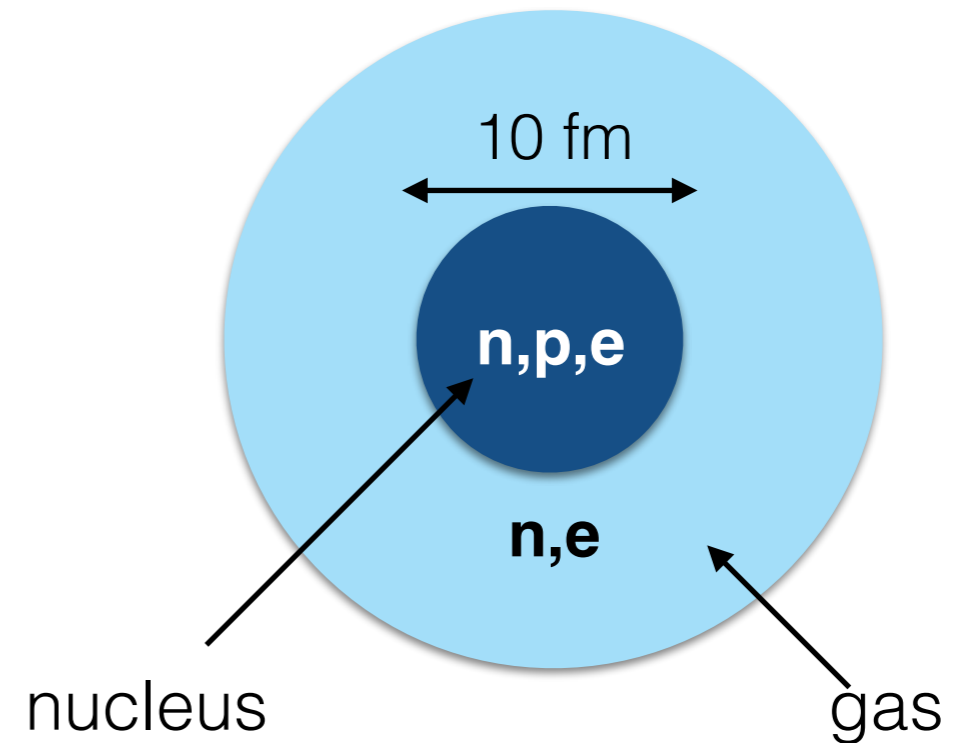
Neutrino Spectra are Sensitive to Symmetry Energy



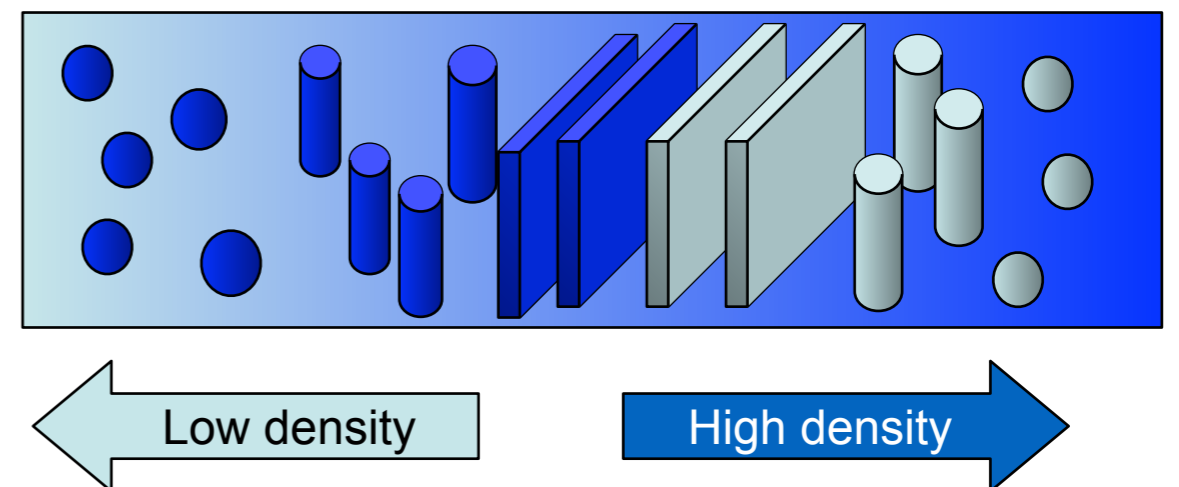
Time evolution of electron neutrino spectrum could be a useful diagnostic. Larger difference between electron and anti-electron neutrino energies is good for the r-process.

10^{13} - 10^{14} g/cm³ and $T \sim 3$ - 20 MeV

- Interesting regime where matter behaves as a dense heterogeneous liquid.
- Virial expansion fails. No small expansion parameter.
- Coexistence between neutron-rich nuclei and neutron-rich matter is favored at lower temperature - favors large density fluctuations.
- Neutrinos can coherently scatter of the heterogeneous structures.



$$\frac{d\Gamma_{\text{coh}}}{d\cos\theta} = \frac{G_F^2 E_\nu^2}{8\pi} n_A (1 + \cos\theta) S(q) N_w^2 F_A^2(q)$$

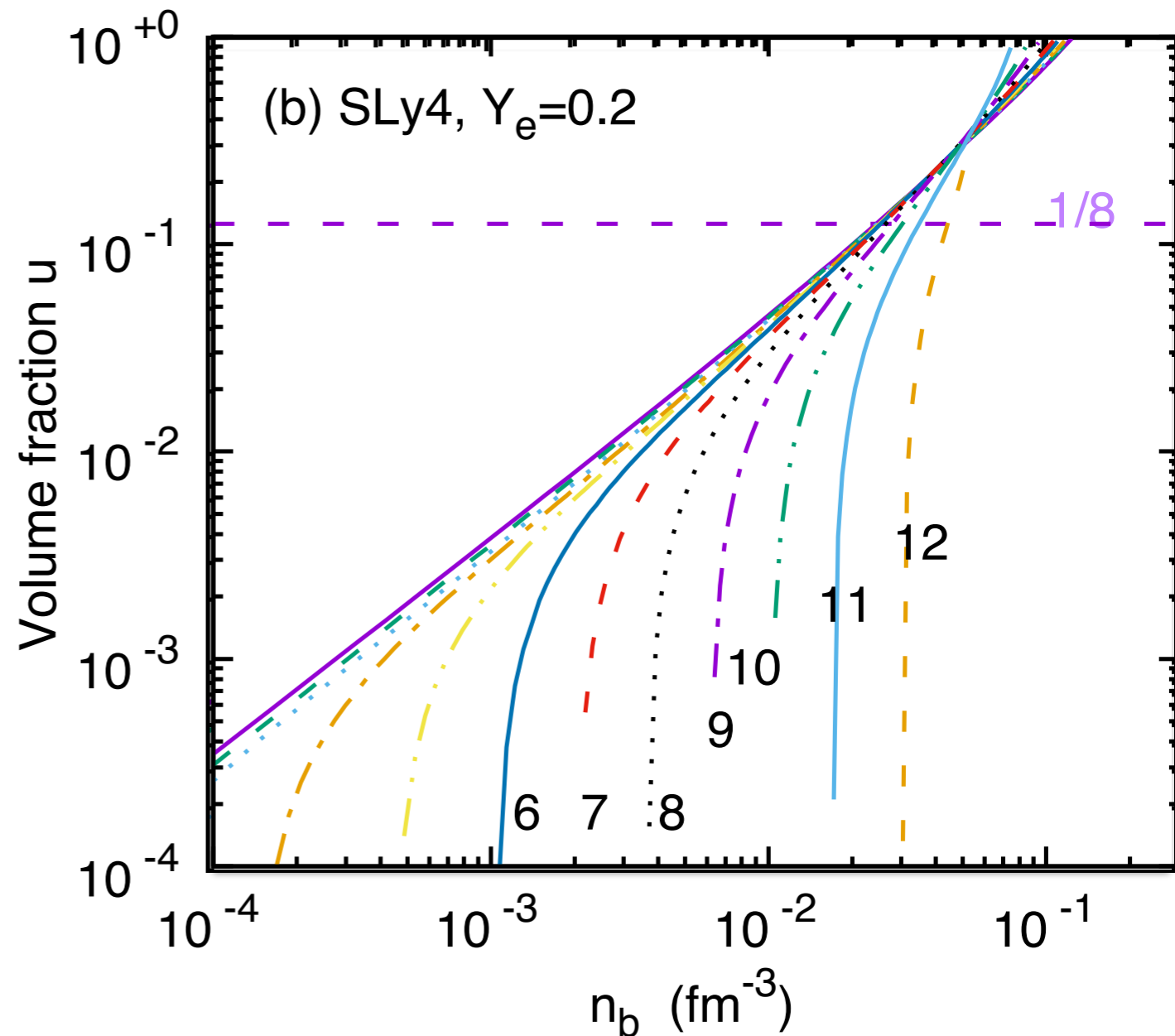


Pasta in Beta-Equilibrium Dissolves at Low Temperature

For large Y_e the volume fraction of nuclei denoted by u is large near the transition density. For small Y_e u decreases rapidly with T as protons leak out of nuclei.

Gibbs equilibrium is altered due to thermal protons in the low-density phase.

Pasta configurations favored at large Y_e at $T=0$, are not realized at $T > 1$ MeV for matter close to beta-equilibrium.

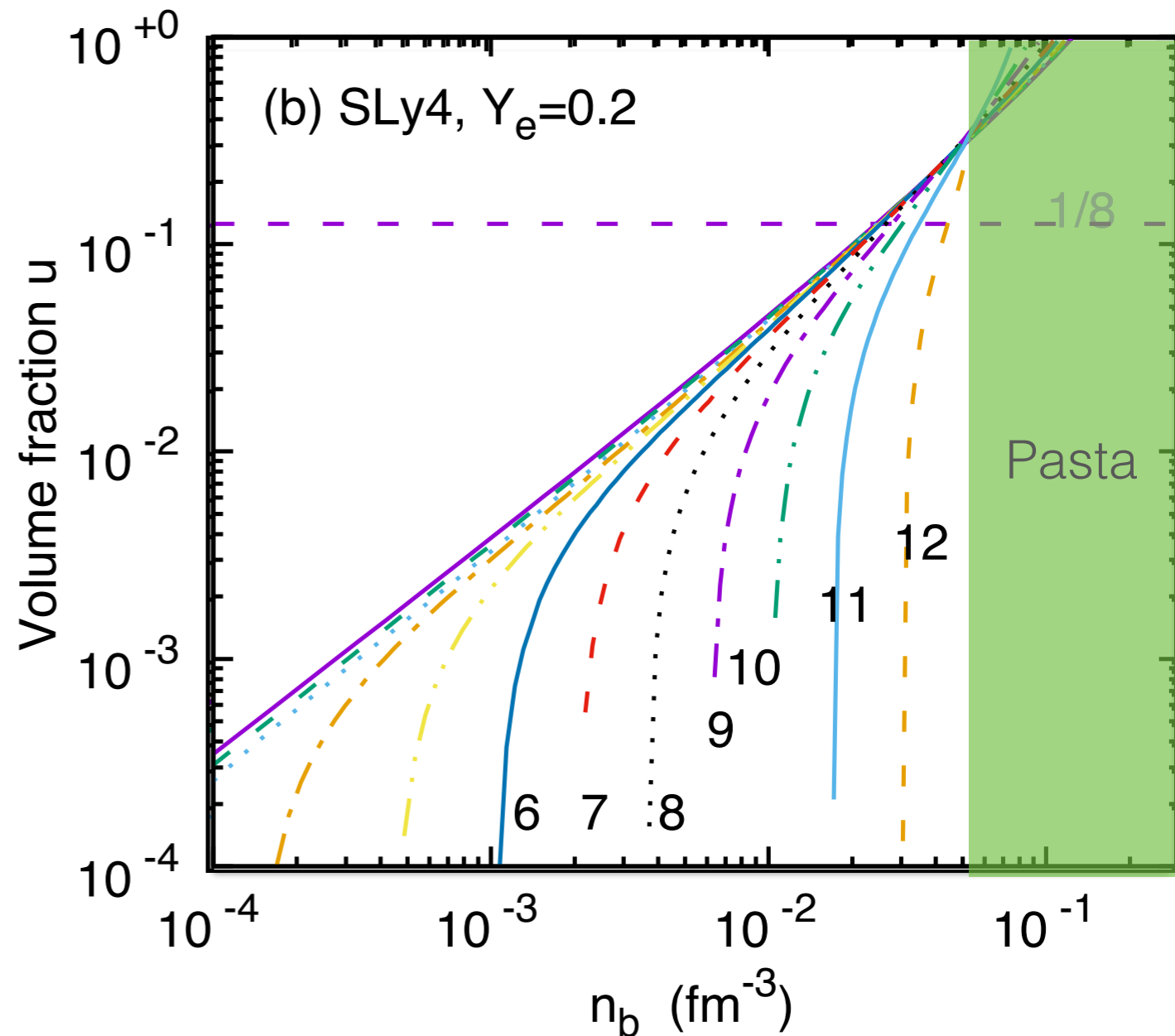


Pasta in Beta-Equilibrium Dissolves at Low Temperature

For large Y_e the volume fraction of nuclei denoted by u is large near the transition density. For small Y_e u decreases rapidly with T as protons leak out of nuclei.

Gibbs equilibrium is altered due to thermal protons in the low-density phase.

Pasta configurations favored at large Y_e at $T=0$, are not realized at $T > 1$ MeV for matter close to beta-equilibrium.

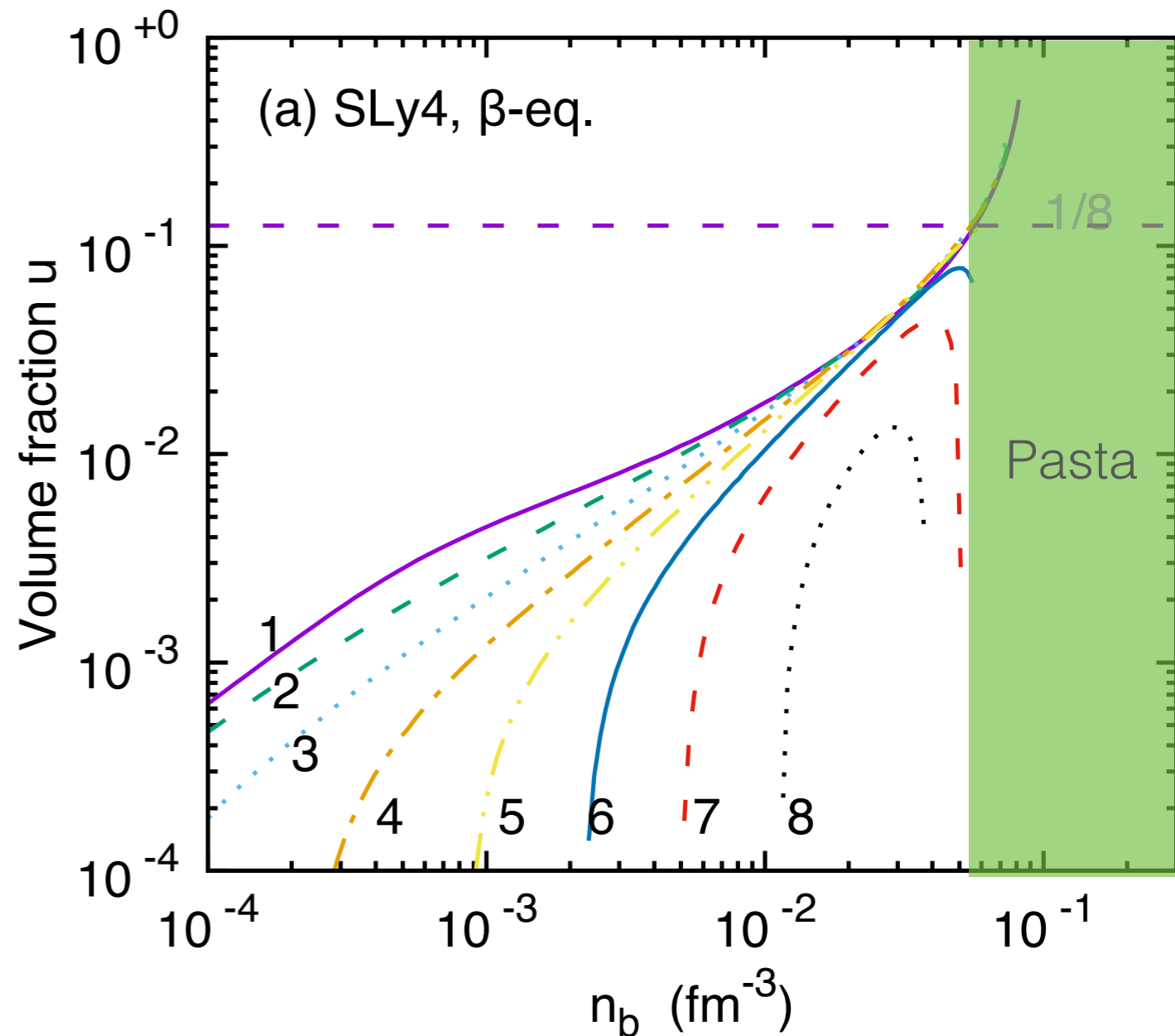


Pasta in Beta-Equilibrium Dissolves at Low Temperature

For large Y_e the volume fraction of nuclei denoted by u is large near the transition density. For small Y_e u decreases rapidly with T as protons leak out of nuclei.

Gibbs equilibrium is altered due to thermal protons in the low-density phase.

Pasta configurations favored at large Y_e at $T=0$, are not realized at $T > 1$ MeV for matter close to beta-equilibrium.

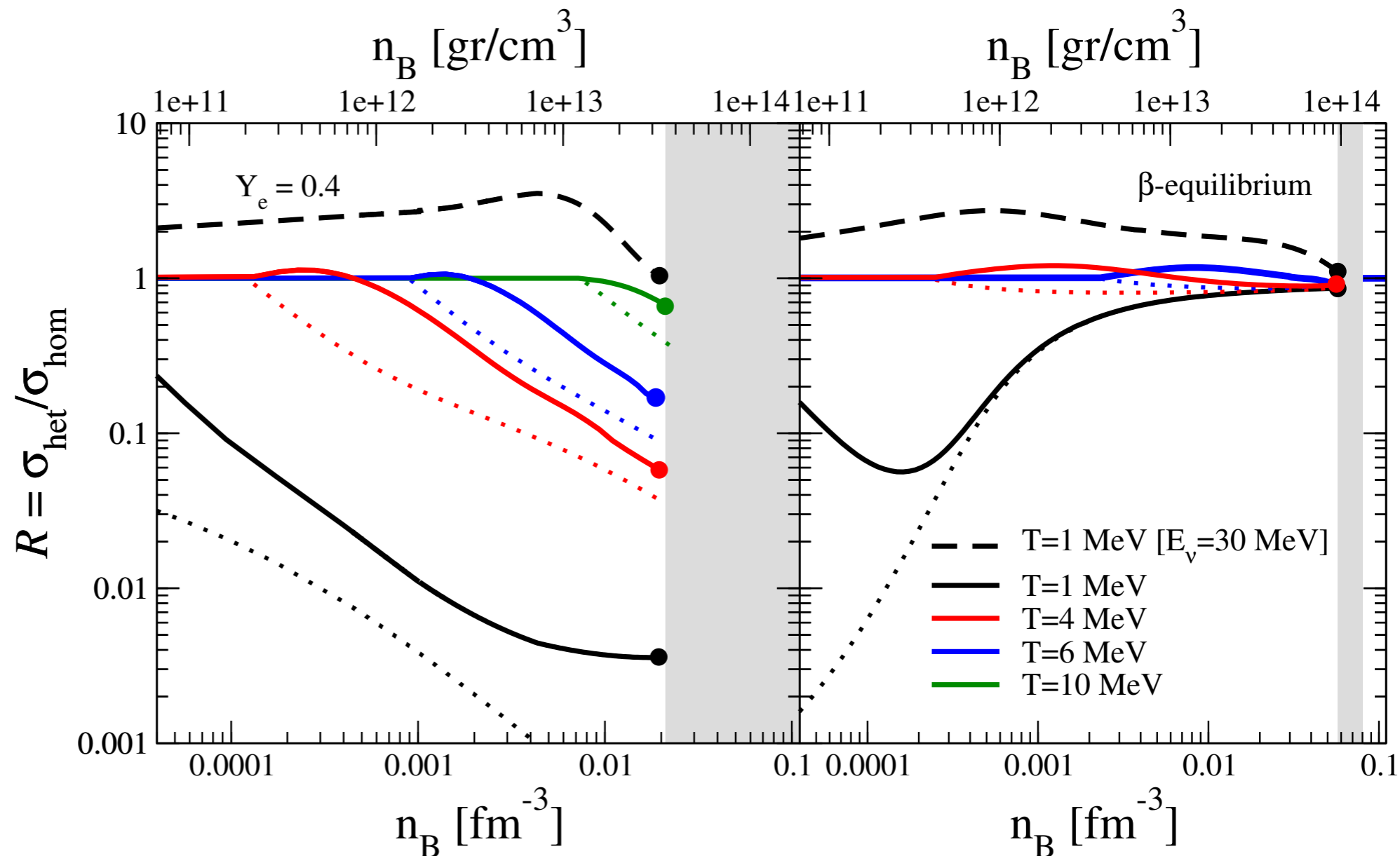


Paucity of Large Nuclei & Reduced Coherent Scattering

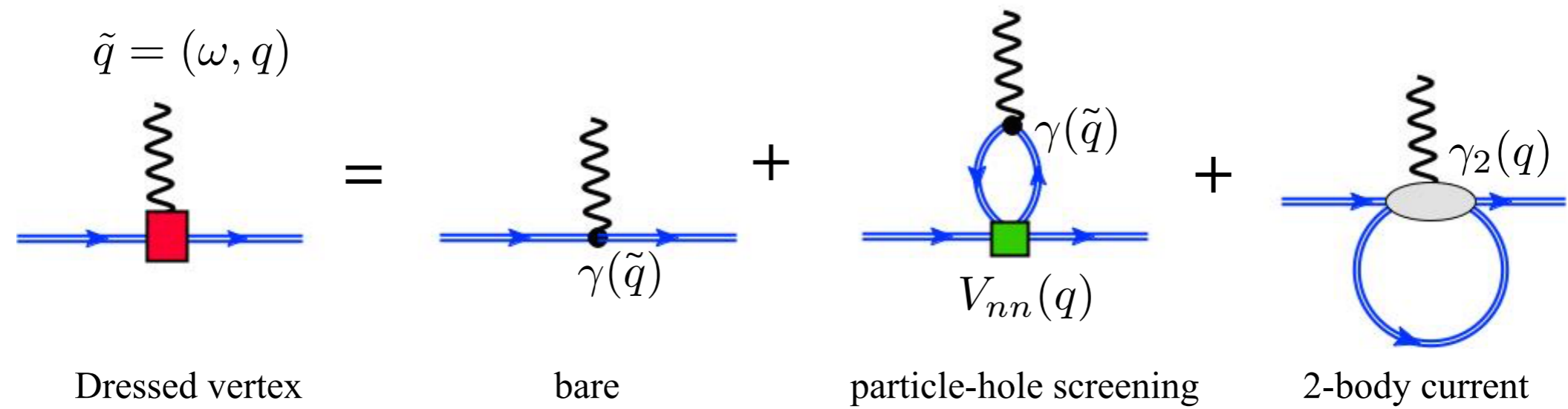
Coherent scattering makes a modest contribution to the total opacity at sub-nuclear density

$$\mathcal{R} = \frac{\sigma_{het}^{tran}(E_\nu)}{\sigma_{hom}^{tran}(E_\nu)} = \frac{\sigma_{coh}^{tran}(E_\nu) + \sigma_{gas}^{tran}(E_\nu)}{\sigma_{hom}^{tran}(E_\nu)} = \frac{n_A N_w^2 \langle S_{cl}(E_\nu) \rangle + (1 + 5(C_A^n)^2) S_{gas}(\mu_n^{het}, T) + 5(C_A^p)^2 S_{gas}(\mu_p^{het}, T)}{(1 + 5(C_A^n)^2) S_{gas}(\mu_n^{hom}, T) + 5(C_A^p)^2 S_{gas}(\mu_p^{hom}, T)}$$

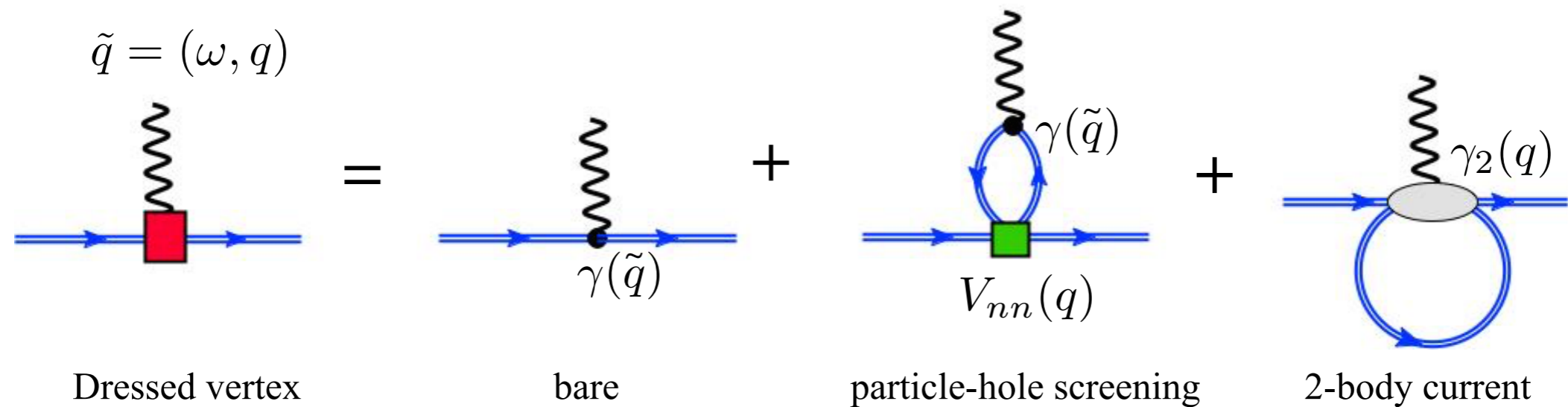
Coulomb
Correlations
between nuclei /
pasta reduces
the response.
Heterogeneous
phase is a low-
pass filter !



10^{14} g/cm³ uniform neutron-rich matter

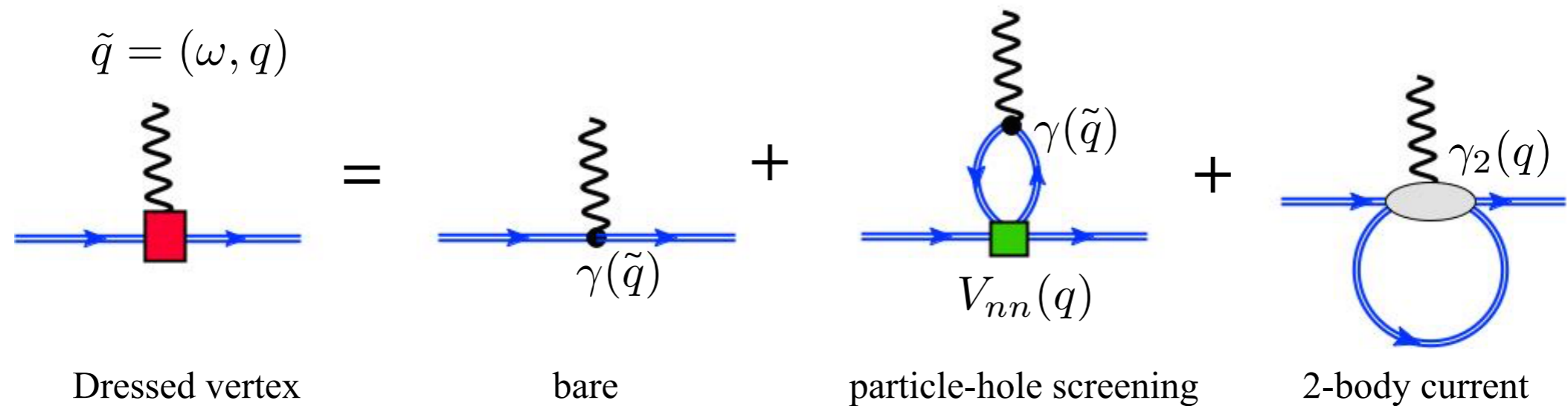


10^{14} g/cm³ uniform neutron-rich matter

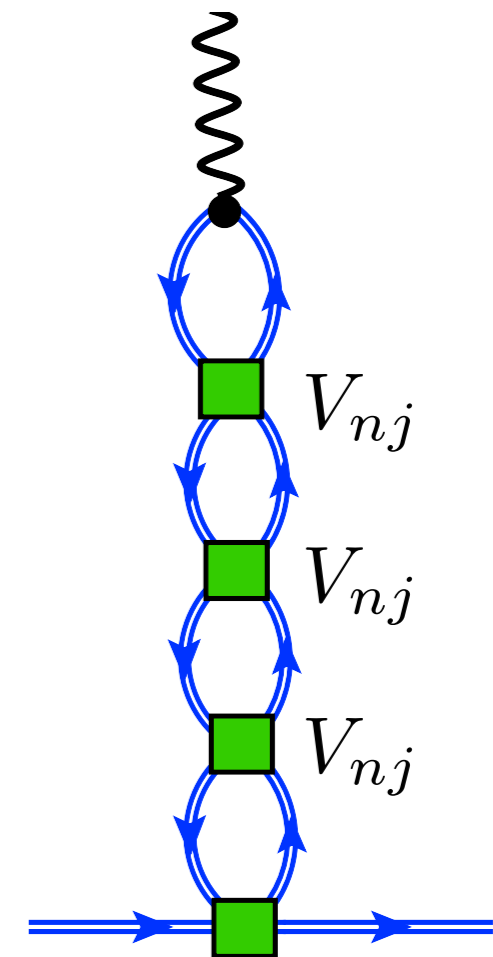


- Corrections due to screening, 2-body currents and 2p-2h excitations are all large. No expansion parameter - results rely on (uncontrolled) many-body approximations.
- Need re-summations - Random Phase Approximation or RPA.
- A lot of work in this direction suggests that both the density and spin response is reduced by factors of 2-4.

10^{14} g/cm³ uniform neutron-rich matter



- Corrections due to screening, 2-body currents and 2p-2h excitations are all large. No expansion parameter - results rely on (uncontrolled) many-body approximations.
- Need re-summations - Random Phase Approximation or RPA.
- A lot of work in this direction suggests that both the density and soon response is reduced by factors of 2-4.



Spin-Response of Neutron Matter: Guidance from Quantum Monte Carlo

Going beyond RPA: Sum-rules can be calculated with QMC.

$$S_{\sigma}^n = \int_{-\infty}^{\infty} d\omega \omega^n S(\omega, q \simeq 0) \quad \bar{\omega}_0 = \frac{S_{\sigma}^0}{S_{\sigma}^{-1}} \quad \bar{\omega}_1 = \frac{S_{\sigma}^1}{S_{\sigma}^0}$$

Density (fm ⁻³)	S_{σ}^{-1} (MeV ⁻¹)	S_{σ}^0	S_{σ}^{+1} (MeV)	$\bar{\omega}_0$ (MeV)	$\bar{\omega}_1$ (MeV)
$n = 0.12$	0.0057(9)	0.20(1)	8(1)	35(9)	40(8)
$n = 0.16$	0.0044(7)	0.20(1)	11(1)	46(11)	55(8)
$n = 0.20$	0.0038(6)	0.18(1)	14(1)	47(12)	78(10)

Shen, Gandolfi, Carlson, Reddy (2012)

In the vicinity of nuclear density QMC sum-rules indicate significant strength at

$$\omega \simeq 30 - 50 \text{ MeV}$$

Spin-Response of Neutron Matter: Guidance from Quantum Monte Carlo

Going beyond RPA: Sum-rules can be calculated with QMC.

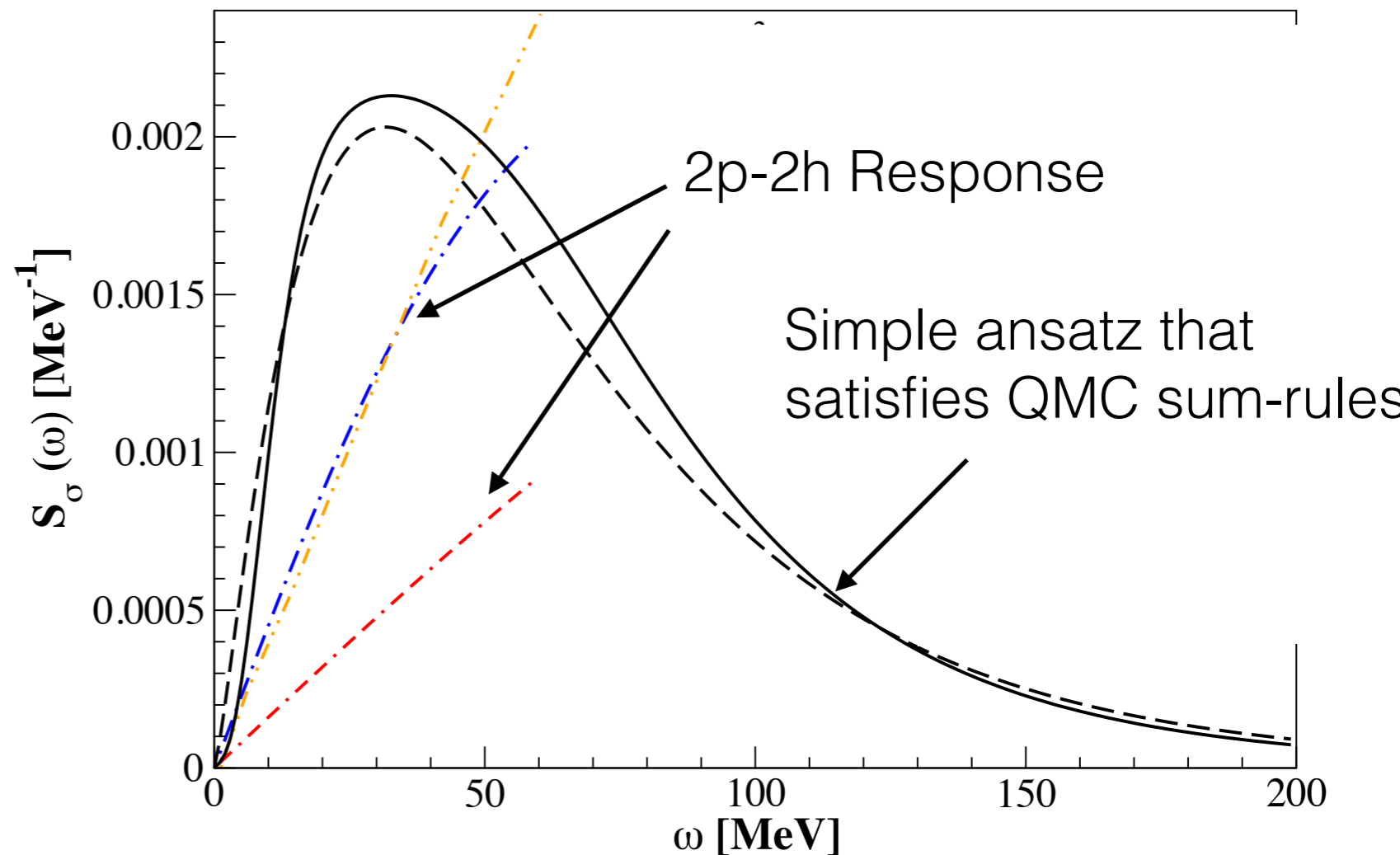
$$S_{\sigma}^n = \int_{-\infty}^{\infty} d\omega \omega^n S(\omega, q \simeq 0) \quad \bar{\omega}_0 = \frac{S_{\sigma}^0}{S_{\sigma}^{-1}} \quad \bar{\omega}_1 = \frac{S_{\sigma}^1}{S_{\sigma}^0}$$

Density (fm ⁻³)	S_{σ}^{-1} (MeV ⁻¹)	S_{σ}^0	S_{σ}^{+1} (MeV)	$\bar{\omega}_0$ (MeV)	$\bar{\omega}_1$ (MeV)
$n = 0.12$	0.0057(9)	0.20(1)	8(1)	35(9)	40(8)
$n = 0.16$	0.0044(7)	0.20(1)	11(1)	46(11)	55(8)
$n = 0.20$	0.0038(6)	0.18(1)	14(1)	47(12)	78(10)

In the vicinity of nuclear density QMC sum-rules indicate significant strength at

$$\omega \simeq 30 - 50 \text{ MeV}$$

Shen, Gandolfi, Carlson, Reddy (2012)



Spin-Response of Neutron Matter: Guidance from Quantum Monte Carlo

Going beyond RPA: Sum-rules can be calculated with QMC.

$$S_{\sigma}^n = \int_{-\infty}^{\infty} d\omega \omega^n S(\omega, q \simeq 0) \quad \bar{\omega}_0 = \frac{S_{\sigma}^0}{S_{\sigma}^{-1}} \quad \bar{\omega}_1 = \frac{S_{\sigma}^1}{S_{\sigma}^0}$$

Density (fm^{-3})	S_{σ}^{-1} (MeV^{-1})	S_{σ}^0	S_{σ}^{+1} (MeV)	$\bar{\omega}_0$ (MeV)	$\bar{\omega}_1$ (MeV)
$n = 0.12$	0.0057(9)	0.20(1)	8(1)	35(9)	40(8)
$n = 0.16$	0.0044(7)	0.20(1)	11(1)	46(11)	55(8)
$n = 0.20$	0.0038(6)	0.18(1)	14(1)	47(12)	78(10)

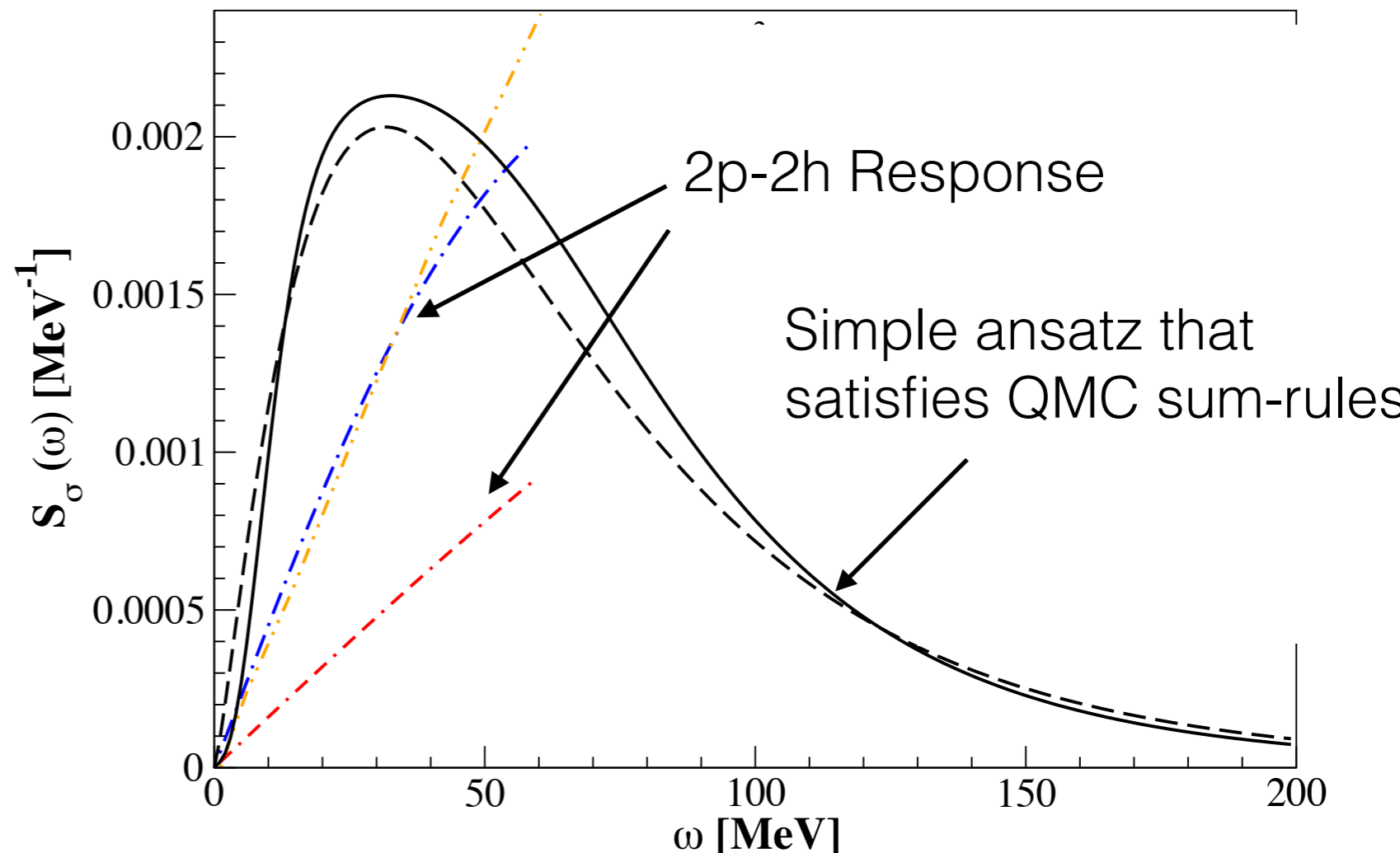
In the vicinity of nuclear density QMC sum-rules indicate significant strength at

$$\omega \simeq 30 - 50 \text{ MeV}$$

Energy scale is large compared to

$$\frac{q^2}{2m} \quad \text{or} \quad q \times v_F$$

Shen, Gandolfi, Carlson, Reddy (2012)



Conclusions

- Effects due nuclear interactions on the density, spin and isospin susceptibility impacts neutrino transport and spectra in supernovae and mergers. Affects SN and BNS mergers: explosion mechanism, nucleosynthesis, mass ejection, and detections.
- First steps towards an ab-initio approach to calculating the dynamic structure factors at densities and temperatures of interest to the neutrino-sphere are encouraging.
- Nuclei and coherent neutrino scattering are reduced in hot neutron-rich matter at small Y_e . Pasta dissolves rapidly.
- At high density sum rules from ab initio theory can be useful to construct reliable models for the dynamic response.
- It is essential to ensure consistency between the EoS and neutrino opacities in simulations.